RSC Advances

REVIEW

View Article Online
View Journal | View Issue

Cite this: *RSC Adv.*, 2024, **14**, 40141

Overview of recent developments in carbon-based nanocomposites for supercapacitor applications

Esmail Vessally, *[ab] Rovnag M. Rzayev,[b] Aytan A. Niyazova,[b] Tushar Aggarwal[c] and Konul E. Rahimova[b]

Received 29th November 2024
Accepted 5th December 2024

DOI: 10.1039/d4ra08446b

rsc.li/rsc-advances

Energy storage devices are recognized as environmentally friendly technologies. Supercapacitors, known for their high cycle stability, have been proposed as potential alternatives to fossil fuels. Recent studies have focused on selecting suitable electrode materials to achieve energy storage systems with high stability, high specific capacity, and biocompatibility. In particular, carbon-based electrode materials, such as graphene oxide, activated carbon, carbon nanotubes, and carbon-based quantum dots, have attracted considerable attention due to their intrinsic properties, such as high conductivity and stability. However, carbon materials alone exhibit limitations, such as low energy density and low specific capacitance. To address this limitation, the synergistic effect of carbon materials has been combined with other electroactive materials to develop electrode materials with enhanced supercapacitor properties. The present study also investigates the supercapacitor performance of carbon-based nanocomposites. It examines the effect of each carbon material (AC, CNT, GO, rGO) on improving the performance of other electroactive materials, including metal oxides, metal sulfides, MXenes, MOFs, and conductive polymers. This study provides valuable insights for further studies on carbon-based electrode materials for supercapacitor applications.

1. Introduction

With the growth of industry, the demand for fossil fuels has increased. However, the limited supply of these resources, along with the resulting environmental pollution from their combustion, has prompted the need for alternative energy generation and efficient energy storage solutions.[1–3] Therefore, suitable alternative technologies to fossil fuels are necessary.[4] As efficient energy storage devices, batteries,[5] fuel cells,[6] and supercapacitors have great potential and have been introduced as alternatives to fossil fuels.[1,7,8] In other words, fuel cells, batteries, and supercapacitors, as electrochemical energy storage technologies, have received much attention as alternatives to fossil fuels in the last few decades.[9–11] Fuel cells are open systems, where the cathodes are responsible for carrying out charge transfer within the system.[12–14] In contrast, batteries and supercapacitors are closed systems, where the mass of the active material in the electrodes participates in redox reactions.[15–17] Supercapacitors, however, do not necessarily involve redox reactions; energy storage is often achieved through the electrical double layer.[18] Supercapacitor devices, as energy storage solutions, offer several key advantages, such as higher energy density than capacitors and higher power density than batteries.[19,20] The typically long lifespan of supercapacitors has led to their extensive use in industry.[21] In contrast, batteries may exhibit weaker performance due to reduced power density caused by Faraday reactions.[22] Therefore, the use of batteries in industrial applications has limitations, although in some cases, batteries are still used in systems that require high energy density.[23] The limitations of using batteries and supercapacitors can be addressed through two general solutions.[24] The first approach involves the fabrication of a hybrid system, combining an electrode with pseudocapacitive properties (*e.g.*, metal oxides, metal sulfides, conductive polymers) and an electrode with double electric layer properties (*e.g.*, carbon materials, including graphene, activated carbon).[25] The second approach utilizes a two-terminal device, incorporating both a battery electrode and a capacitor electrode.[26] Connecting a supercapacitor device to a battery can improve the battery performance, including increasing its life and decreasing voltage instability.[27,28] The performance of the supercapacitor device depends on the type of electrode material used, so a smart choice of the electrode material is important for achieving an efficient supercapacitor device.[29] Commonly used electrode materials in supercapacitors include metal oxides,[30] metal sulfides,[31] conductive polymers,[32] quantum dots,[33] and metal–organic frameworks (MOFs).[34] However, these materials used for constructing supercapacitors have limitations too. Consequently, nanocomposites based on carbon compounds have been synthesized to improve the final performance and attain electrode materials with a high specific surface area, better conductivity, and high specific capacitance.[35]

[a]*Department of Chemistry, Payame Noor University, Tehran, Iran. E-mail: vessally@yahoo.com*

[b]*Composite Materials Scientific Research Center of Azerbaijan State University of Economics (UNEC), 194 M. Mukhtarov str. Baku, Azerbaijan*

[c]*Centre for Research Impact & Outcome, Institute of Engineering and Technology, Chitkara University, Rajpura, 140401, Punjab, India*

Carbon materials that have been investigated as electric double-layer capacitors (EDLCs) in supercapacitor systems include activated carbon, carbon nanotubes, and graphene oxide.[36] These materials alone have low energy density and low specific capacitance,[37] but compositing these materials with *e.g.*, metal oxides,[38,39] metal sulfides,[40] MOFs,[41] and conductive polymers increases their specific surface area and performance.[42] Therefore, the compositing of carbon materials with other materials with pseudocapacitive properties can allow obtaining electrode materials with optimal performance.[42] Increasing the specific surface area increases the rate of penetration of electrolyte ions, resulting in a shortening of the ion-diffusion pathways.[43,44] In this study, our team reviewed recent research on the supercapacitor performance of carbon-based nanocomposites. Specifically, by investigating recent studies on the supercapacitor performance of various carbon-based nanocomposites (carbon/TMO materials, carbon/TMS materials, carbon/conductive polymer materials, carbon/MOF materials, and carbon/MXene materials), the effect of the carbon materials on improving the performance of each quasi-capacitor material was determined.

2. Supercapacitor devices

Supercapacitor systems can be divided into three categories based on the charge-storage mechanism:[45] electrochemical double layer (the charge accumulates in the interface between the electrodes),[46,47] pseudocapacitors (storage is done through a reversible surface redox process),[48] and hybrid capacitors (combination of double electric layer and pseudocapacitor).[49]

2.1. EDLCs

EDLCs were discovered at the beginning of the 15th century during the study of opposite charges located at the interface of colloidal particles.[50] The performance of EDLCs is similar to that of common capacitors, but EDLCs have a higher energy density than capacitors.[51] Conventional capacitors are made of a dielectric medium, but in EDLCs, an electrolyte is located between the two electrode layers.[52] The energy-storage mechanism of EDLCs is physical. Then, during discharge, electrons move from the negative terminal to the positive terminal, which separates the cations and anions from the surface of the electrons, and so charge transfer does not occur at the electrode/electrolyte interface.[53] Three general models were proposed to define the structure of EDLCs (Fig. 1). The first model was proposed by Helmholtz in the 19th century, in which opposite charges accumulate at the interface of the electrode and the electrolyte, and the two plates are separated by a distance similar to in a capacitor. A second model was introduced by Gouy and Chapman, in which a diffusion layer is considered and the specific capacitance increases as the charges approach each other. A third model was proposed by Stern combining the two earlier models (Helmholtz's model and Gouy and Chapman's model), which considers a compressed layer (the Stern layer).[55] The commonly used electrode materials for EDLC supercapacitors are carbon materials with a high specific surface area and promising electrical conductivity, including activated carbon, graphene, and carbon nanotubes.[53]

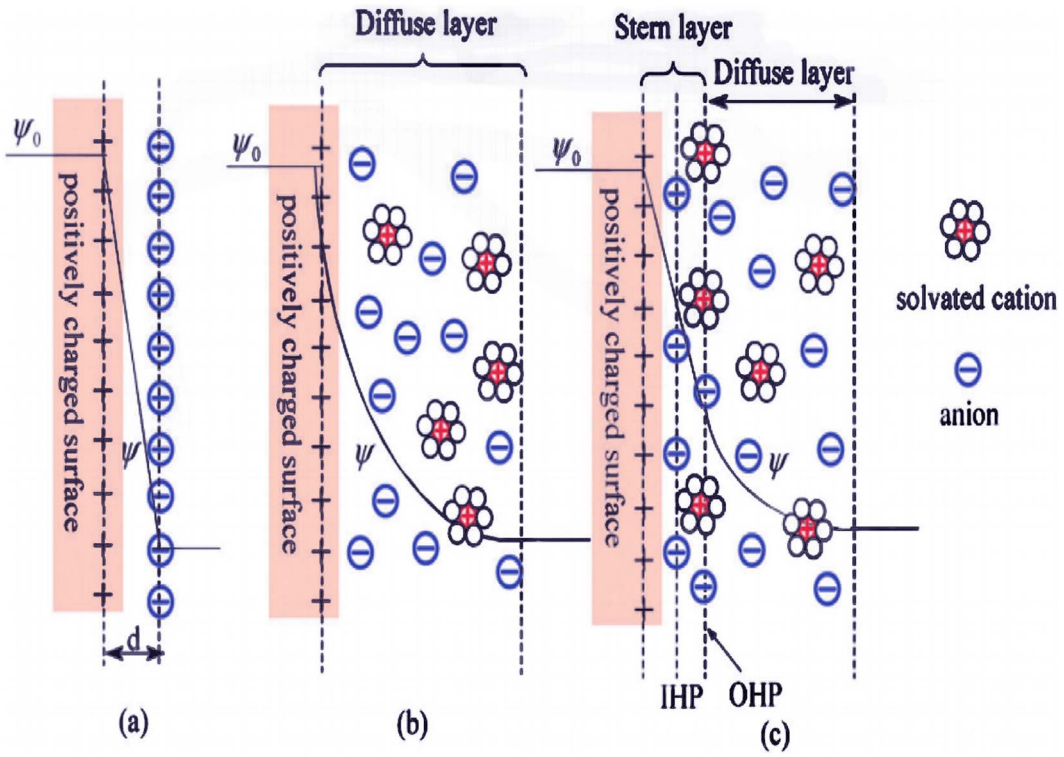

Fig. 1 Models for the electrical double layer at a positively charged surface: (a) the Helmholtz model, (b) the Gouy–Chapman model, and (c) the Stern model.[54]

2.2. Pseudocapacitors

The charge-storage mechanism of pseudocapacitors is faradaic, whereby electron transfer is carried out through the oxidation and reduction of a chemical substance.[56] This process can be reversible or irreversible. In the reversible process, the redox reaction is imposed on the electrode surface by applying voltage, which causes the electrolyte ions to diffuse from the solution to the electrode material. Then, the ions of the electrode material return to the electrolyte at the time of discharge. The performance and the specific capacitance of pseudocapacitors depend on the electrode morphology. For example, molybdenum oxide can be synthesized as alpha and beta phases under different conditions, including different temperatures and reaction times. The alpha phase has a sheet or rod morphology while the beta phase has a spherical morphology. The sheet morphology has a larger specific surface area, which allows for a higher specific capacitance.[57,58] Pseudocapacitors have a higher specific capacitance than EDLCs, but the stability of pseudocapacitors is lower than EDLCs due to their reliance on faradaic reactions and their shorter cycle life. The general process of pseudocapacitors is voltage-dependent due to the charge-transfer mechanism depending on the voltage.[59] Metal oxides, conductive polymers, and metal sulfides are some common electrode materials with pseudocapacitor properties. However, while they have high capacitance, they are generally less stable in charge–discharge cycles.

2.3. Hybrid capacitors

Hybrid devices are intermediates or combinations of EDLCs and pseudocapacitors.[60] Hybrid devices are classified into three general categories. The first category is composites, which are fabricated from a combination of carbon materials (graphene, carbon nanotubes, and activated carbon) and pseudocapacitor materials (metal oxides, metal sulfides, and conductive polymers). Composite electrode materials can be used as symmetric or asymmetric systems. In asymmetric systems, composite and carbon materials are used as the positive and the negative electrodes, respectively. The second category is asymmetric devices, which utilize pseudocapacitor materials (metal oxides, conductive polymers) as positive electrodes and carbon materials (graphene, CNT, and active carbon) as negative electrodes. The third category is asymmetric supercapacitors of the battery type. In this type of asymmetric supercapacitor, the positive electrode is a battery material and the negative electrode is a capacitor material.[61] The operation of a battery-type supercapacitor in non-ionic electrolytes occurs *via* several stages. In the first stage, during charging, the negative ions of the electrolyte move toward the positive electrode, and the positive ions of the electrolyte move toward the negative electrode (the volume of ions thus decrease in the electrolyte solution). In the second stage, the ions return to the electrolyte upon discharge, and the volume of ions in the electrolyte solution thus increases. In the third stage, the concentration of negative ions in the electrolyte is constant and the positive ions move toward the positive electrode. Therefore, a constant concentration of positive and negative ions remain in the electrolyte.[53]

2.4. Supercapacitor techniques

To evaluate the quality of supercapacitors, it is necessary to check certain parameters, such as the specific capacitance, current density, power density, and stability. Therefore, reliable techniques are needed to evaluate these parameters. Using the following three techniques, the electrochemical properties of the supercapacitor can be checked.[62]

2.4.1 Cyclic voltammetry. Cyclic voltammetry (CV) analysis can be used to check the electrochemical behavior of an electrode material. When the applied voltage is higher than the predicted voltage, the current can be checked using CV analysis (Nernst equation).[63] In CV analysis, the electrochemical behavior during the forward and the reverse scan is investigated, which can be distinguished from the pseudocapacitor behavior according to the observed peaks and the general shape of the EDLC behavior diagram for the electrode material.[64] This technique examines the material's electrochemical behavior by using working, reference, and counter electrodes in a three-electrode setup in supercapacitor systems.[65] The main limitation of cyclic voltammetry is that the thermodynamic aspect is ignored and only the kinetic aspect of the material is considered. The specific capacitance can be calculated using the cyclic voltammetry technique with eqn (1).[66]

$$C = \frac{\int iV \, dV}{2\mu m \, \Delta V} \tag{1}$$

where i, V, m, and ν are the current density, potential region, mass of active materials, and scan rate, respectively.[67]

2.4.2 Galvanostatic charge/discharge. Galvanostatic charge and discharge analysis examines changes in the potential over time. In this analysis, the electrode material is charged and discharged at a certain time according to the properties of the material type (specific surface, electrical activity, *etc.*).[68] The specific capacity, power density, stability, and energy balance are calculated from the data related to the potential window and the charge and discharge time.[69] The general shape of the charge–discharge diagram shows the difference between EDLC and pseudocapacitor behaviors according to the shoulders created by the faradaic currents. Eqn (2)–(4) can be used in galvanostatic charge and discharge analysis to calculate the specific capacity, current density, and power density.[70]

$$C = 4C_{\text{cell}} = \frac{I\Delta t}{m\Delta V} \tag{2}$$

$$E = \frac{1}{2} C_{\text{cell}} \times \Delta V^2 \times \frac{1}{3.6} \tag{3}$$

$$P = \frac{E}{\Delta T} \times 3600 \tag{4}$$

where C_{cell} (F g^{-1}), m, Δt, E, ΔV, and I are the specific capacitance, total mass of active material, discharge time, energy density, discharge current density, and potential window, respectively.[71]

2.4.3 Electrochemical impedance spectroscopy (EIS). Impedance analysis can be performed to evaluate the required parameters of supercapacitor devices. The data from

impedance analysis are usually processed by suitable software, such as ZView, so an equivalent circuit can be defined for this analysis.[72] The elements of this equivalent circuit show the general characteristics of the supercapacitor, such as the equivalent series resistance, the supercapacitor's non-ideal behavior, and the charge-transfer capacitance. Using the results of the impedance analysis, the specific capacitance can be calculated using eqn (5).[73]

$$C = \frac{1}{(2\pi f|Z|)} \quad (5)$$

where $|Z|$ and f are the imaginary part of the impedance, and the frequency.

3. Carbon materials

The use of carbon materials with a high specific surface area as a conductive component in carbon-based nanocomposites can improve the performance of other materials (metal oxides, MOFs, metal sulfides, and conductive polymers). In the following, we review different types of carbon materials.[74,75]

3.1. Carbon onions

Carbon onions are carbon skins with a spherical morphology that were first introduced as carbon nano-onions (CNOs) and later called onion-like carbon (OLC). OLC was discovered by chance in a transmission electron microscopy (TEM) image in 1980 in Sumio Iijima's study investigating carbon black.[76] It was later found that OLC with the sp^2 network structure allows passing loads faster.[77] These materials (OLCs) were later used as EDLC electrode materials in the construction of supercapacitors, and it was found that, compared to other EDLC materials, the energy-storage performance did not have a temperature limit and hence they could be used in a wider temperature range.[78] Various synthesis methods have been used to prepare OLCs, including the annealing method and arc-discharge method, which have made large-scale production possible.[76] In general, the low cost of OLC synthesis has led to the wide use of these materials in industry.[79] The energy density of these materials is up to 10 W h kg^{-1}, which requires activation. Indeed, with activation, the specific capacitance of OLCs increases. However, the activation of OLCs leads to a decrease in the quality of these materials. The use of OLCs as anodes and other pseudocapacitor materials as cathodes in asymmetric supercapacitors can lead to efficient energy-storage systems with a high power density and high energy density.[80]

3.2. Activated carbon

Activated carbon is a suitable and promising material for use in energy-storage systems. Activated carbon is prepared by chemical (at low temperature in the presence of chemicals such as potassium hydroxide) and physical methods (at high temperature in the presence of carbon dioxide in air).[81,82] Studies have been done to improve the electrochemical performance and increase the specific surface of these materials.[83,84] Activated carbon can be obtained from various sources, such as sugarcane waste,[85,86] coconut cellulose,[87] and figs, among which the activated carbon obtained from fig wastes has demonstrated good electrochemical performance (high specific surface area).[88] Activated carbon electrode materials offer ideal performance in aqueous electrolytes and organic electrolytes because these organic materials create pores with inappropriate sizes (small) that do not participate in the electrochemical mechanism.[89,90]

3.3. Carbon nanotubes (CNTs)

Carbon nanotubes (CNTs), discovered in 1991, offer good performance in supercapacitor energy-storage systems due to their high specific surface area, high electrical conductivity, and chemical stability.[91–93] The carbon nanotube is a graphene sheet in the form of a small tube (nano size).[94,95] Carbon nanotubes can be single-walled (SWNTs),[96] multi-walled (MWNTs),[97] and double-walled (DWNTs).[98] The structure of carbon nanotubes is a height of a few microns and a nano diameter, whose ends are covered with a fullerene structure.[99] There are different methods for the synthesis of the different types of carbon nanotubes.[100–102] For the synthesis of SWNTs and MWNTs, the methods include carbon monoxide thermal decomposition with a laser pulse,[103] and carbon arc discharge.[104,105] Also, plasma-enhanced chemical vapor deposition and chemical vapor deposition have been used for the synthesis of parallel single-walled nanotubes and parallel multi-walled nanotubes, respectively.[106,107] Among the various types of carbon nanotubes, interwoven carbon nanotubes were the first class of nanotubes studied in supercapacitor systems.[108] In addition to intertwined nanotubes, aligned nanotubes have also been used in supercapacitor devices.[109,110] This feature of the alignment of carbon nanotubes makes it easy to access the structure of the nanotubes and improve their performance in energy-storage devices.[111] Although carbon nanotubes have a lower specific surface area than activated carbon, they have a higher specific capacitance; hence many studies have been conducted on the supercapacitor performance of carbon nanotubes.[112] Also, the high specific capacitance of carbon nanotubes compared to activated carbon can be attributed to their high porosity, high conductivity, and upper rate capability.[113] Carbon nanotubes have a high specific capacitance at high frequencies because the transmission capability in carbon nanotubes is high. The power density of CNT electrode materials is higher than that of carbon electrode materials, but the energy density is low, which can be modified through compositing them with other electroactive materials.[114]

3.4. Graphene

Graphene is well known as a monolayer sheet of carbon atoms. In the structure of graphene, each carbon atom has a covalent bond with three adjacent carbons.[115,116] Graphene has special electrical and thermal properties, which are provided by its one free electron.[116] Recently, there has been considerable focus on graphene as a two-dimensional structure with a thick single-atomized layer as an electrode material in supercapacitor systems.[117,118] Graphene electrode materials have a large specific surface, so they have high electrical conductivity and chemical

stability. Therefore this material has been widely investigated and used as a distinctive carbon material in energy-storage and production devices.[4,119] Also, one of the important reasons for using graphene as an electrode material unlike other carbon materials, such as carbon nanotubes, activated carbon, is that it has no distribution of pores in the solid state.[120]

3.5. Graphene oxide (GO)

Graphene oxide is a mixture of carbon, oxygen, and hydrogen in variable proportions, which is obtained by combining graphite with strong oxidizers.[75,121] The product mass that is maximally oxidized is a solid with the formula C : O.[122] The presence of oxygen groups in the structure of graphene oxide endows it with a better ability to interact with various materials. This material can be used in various applications, including supercapacitors.[123] Hydroxyl and epoxide groups can be attached to graphene oxide to enable graphene oxide to connect these sheets with covalent bonds to many materials and polymers.[124] Graphene oxide with a layered structure is one of the most important derivatives of graphene. The layered structure of graphene oxide with a high surface area endows it with suitable supercapacitor properties.[125,126]

4. Nanocomposites based on carbon materials

Selecting suitable electroactive materials for constructing supercapacitors is important for the final behavior of this system as an efficient energy-storage system. Different carbon materials are the first candidate electrode materials for making supercapacitors, which offer high stability but low specific capacitance. These are combined with metal oxides, metal sulfides, polymers, conductive polymers, and MOFs with suitable supercapacitor behavior as candidate electrode materials for the fabrication of supercapacitors.[127] Because the charge-storage mechanism of metal oxides is related to the redox reaction at the electrode/electrolyte interface, they have a high specific capacitance. However, the stability of metal oxides is lower than that of carbon. A suitable method for preparing efficient materials is the synthesis of nanocomposites based on carbon materials and other electroactive materials (metal oxides, metal sulfides, conductive polymers, and MOFs).

4.1. Nanocomposites of carbon materials/metal oxides

Various methods have been used for the synthesis of nanocomposites based on carbon nanotubes and metal oxides, including atomic layer deposition, which typically require a lot of time and cost. Recently, other new methods, including hydrothermal methods, have been used for the synthesis of these nanocomposites. In one study, CNT/Fe_2O_3 nanocomposites with different weight ratios of CNT were synthesized by hydrothermal method. In this study, the supercapacitor behaviors of Fe_2O_3 electrode materials, 5 wt% CNT/Fe_2O_3 nanocomposite electrode materials, and 10 wt% CNT/Fe_2O_3 nanocomposite electrode materials were investigated. The electrochemical analysis of Fe_2O_3 and the nanocomposites revealed that the presence of CNT prevented the aggregation of Fe_2O_3 and increased the conductivity of the nanocomposites. Further investigation of the electrochemical behavior of CNT/Fe_2O_3 nanocomposites with different weight ratios of CNT (5% and 10%) showed that with the increase in the percentage of CNT from 5% to 10%, the dispersion of Fe_2O_3 increased, which caused a rise in the penetration rate of electrolyte ions. Finally, the power density, specific capacitance, and stability of the nanocomposite with 10 wt% of CNT were higher than the nanocomposite with 5 wt%.[128] In another study, a composite based on graphite and carbon nanotubes (CNT/GT composite) was synthesized by a facile method. Then, at three drying temperatures, zinc oxide (ZnO) was sprayed on to the nanocomposite. The supercapacitor behavior of the nanocomposites was investigated in 1 M KOH electrolyte solutions. The results confirmed the optimal supercapacitor behavior for the nanocomposite prepared at 300 °C. This study confirmed that a careful selection of the temperature conditions could effectively allow obtaining nanocomposites based on carbon materials and metal oxides with ideal supercapacitor behavior. Finally, the CNT/GT/ZnO-300 nanocomposite showed a specific capacitance of 6.99 F g^{-1} at a scan rate of 25 mV s^{-1}.[129] To investigate the effect of the type of electrolyte on the final behavior of nanocomposites based on carbon materials and metal oxides, Thakur *et al.* synthesized composites based on reduced graphene oxide and titanium oxide (rGO–TiO_2 composite) and investigated their electrochemical behavior in different electrolytes. The results showed the improvement of the supercapacitor performance of the composite compared to that of the constituent components. Also, the effect of the type of electrolyte on improving the performance of these nanocomposites was investigated. The results showed specific capacitances of 4.89 F g^{-1} in H_2SO_4 electrolyte, 4.89 F g^{-1} in Na_2SO_4 electrolyte, and 1.42 F g^{-1} in KOH electrolyte at the same molarities (1 M) at the same scan rate of 0.05 V s^{-1}.[130] The proportion of carbon materials will influence the final performance of the supercapacitor. Sudarto *et al.* synthesized nanocomposites based on titanium dioxide, activated carbon, and carbon nanotubes (TiO_2/CNT/AC) with different ratios of CNTs (0%, 7%, 14%, and 21%). This investigation showed that the increase in the CNT percentage improved the electrical conductivity.[131] Hye Kim and colleagues synthesized a zinc oxide/activated carbon nanofiber composite through electrospinning. The supercapacitor performance of the zinc oxide/activated carbon nanofiber electrode materials and activated carbon nanofiber electrode materials were investigated in KOH electrolyte. The results confirmed the synergistic effect between ZnO and ACNF. The high surface area of the activated carbon nanofiber together with the high specific capacitance of zinc oxide promoted the good supercapacitor performance of the composite as an electroactive material.[132] Carbon cloth is a suitable substrate for assessing the metal oxide performance in supercapacitor systems. In studies conducted to investigate the performance of hierarchical supercapacitors, Lei *et al.*, using the hydrothermal method, first synthesized $NiCo_2O_4$ with a needle structure on carbon cloth (CC/$NiCo_2O_4$–N@NiO) and $NiCo_2O_4$ with a cut-like structure on carbon cloth (CC/$NiCo_2O_4$–

S/NiO) (Fig. 2). In the next stage, NiO was grown on CC/$NiCo_2O_4$–N@NiO and CC/$NiCo_2O_4$–S/NiO. The CC/$NiCo_2O_4$–N/NiO showed a specific capacitance of 709 F g^{-1} while CC/$NiCo_2O_4$–S/NiO showed a specific capacitance of 775 F g^{-1} at the same current density. By examining the morphology of these two core–shell structures by SEM and TEM images and examining the surface by BET analysis, the presence of multiple pores of different sizes in these structures was confirmed, which are beneficial for increasing the penetration of electrolytes and improving the supercapacitor properties. Electrochemical analyses of these two core–shell structures showed redox peaks that were related to faradaic reactions carried out by the core–shell structures. The electrochemical performance of carbon cloth alone was investigated to investigate the effect of carbon cloth on the final performance of these electrode materials. The results of the comparison of the analyses showed the increase in the subsurface area with the presence of carbon cloth. An asymmetric device was fabricated for both core–shell structures grown on carbon fabric using graphene as a negative electrode. Examining the electrochemical results related to both asymmetric devices showed they were highly stable for up to 1000 cycles.[133]

Liu *et al.* prepared a nanocomposite based on carbon nanotubes, graphite foam, and iron oxide (GF/CNT/Fe_2O_3) as an anode electrode for the manufacture of an asymmetric supercapacitor. According to Fig. 3, carbon nanotubes were first formed on the nickel foam, and then iron oxide was placed on the carbon nanotubes. Investigation of the electrochemical behavior of the GF–CNT/Fe_2O_3 electrode material utilizing a three-electrode systems showed the EDLC behavior of graphite foam and carbon nanotubes with the quasi-capacitive behavior of iron oxide. The performance of the GF–CNT/Fe_2O_3 composite with different Fe_2O_3 ratios (200, 400, and 600) was next investigated. Examining the supercapacitor behavior of the three composites with the different Fe_2O_3 ratios showed that GF/CNT/200Fe_2O_3 had a lower current density than the GF/CNT/400Fe_2O_3 composite. With increasing the percentage of Fe_2O_3 in the GF/CNT/600Fe_2O_3 composite, the ionic conductivity decreased. Therefore, the GF/CNT/400Fe_2O_3 composite was chosen as the negative electrode to make an asymmetric supercapacitor device. Finally, the asymmetric supercapacitor was fabricated using GF/CNT/400Fe_2O_3 composite as the negative electrode and GF $CoMoO_4$ as the positive electrode (Fig. 3). Investigation of the specific capacitance of the asymmetric device (GF–CNT/Fe_2O_3//GF–$CoMoO_4$) at different current densities, as shown in Fig. 3c, revealed that with the increase in the current density, the specific capacitance decreased to a small amount, which confirmed the good supercapacitor behavior of the asymmetric device. Also, the asymmetric device (GF–CNT/Fe_2O_3//GF–$CoMoO_4$) showed 95% stability for up to 5000 cycles. The asymmetric device (GF–CNT/Fe_2O_3//GF–$CoMoO_4$) with high energy density is an example of an efficient supercapacitor device that was able to overcome the limitations of supercapacitor devices by the careful choice of effective electroactive materials[134] (Table 1).

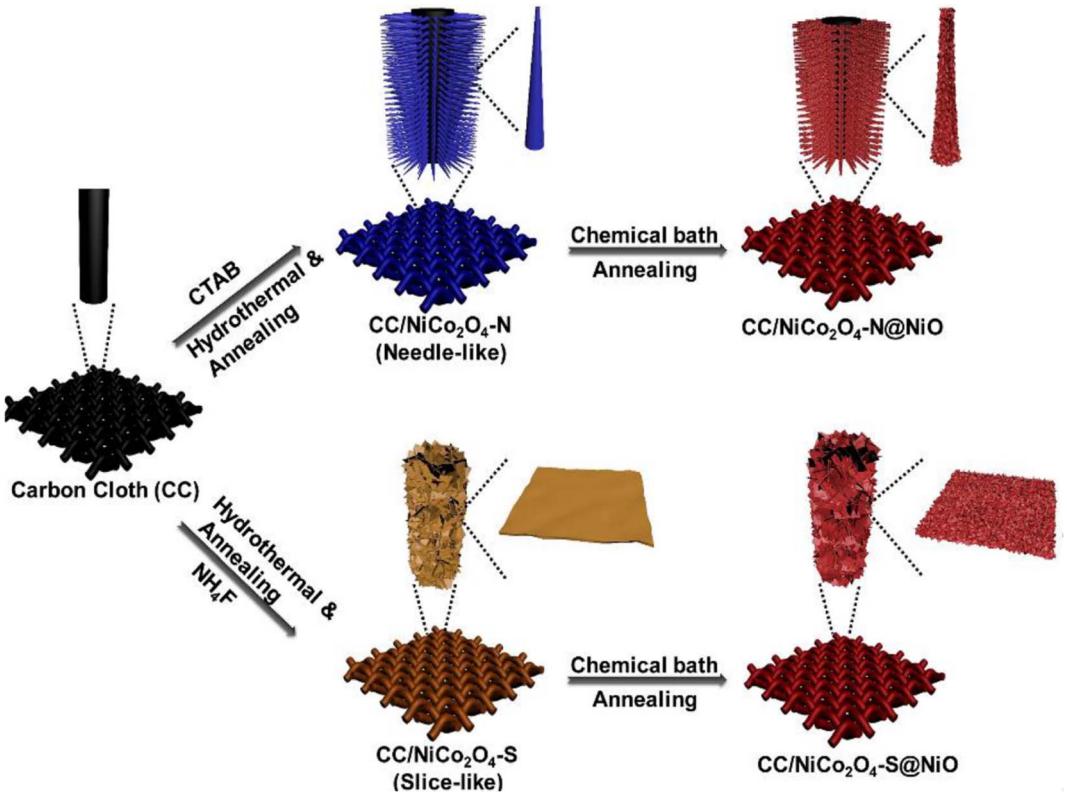

Fig. 2 Schematic of the preparation of CC/$NiCo_2O_4$–N@NiO and CC/$NiCo_2O_4$–S@NiO.[133]

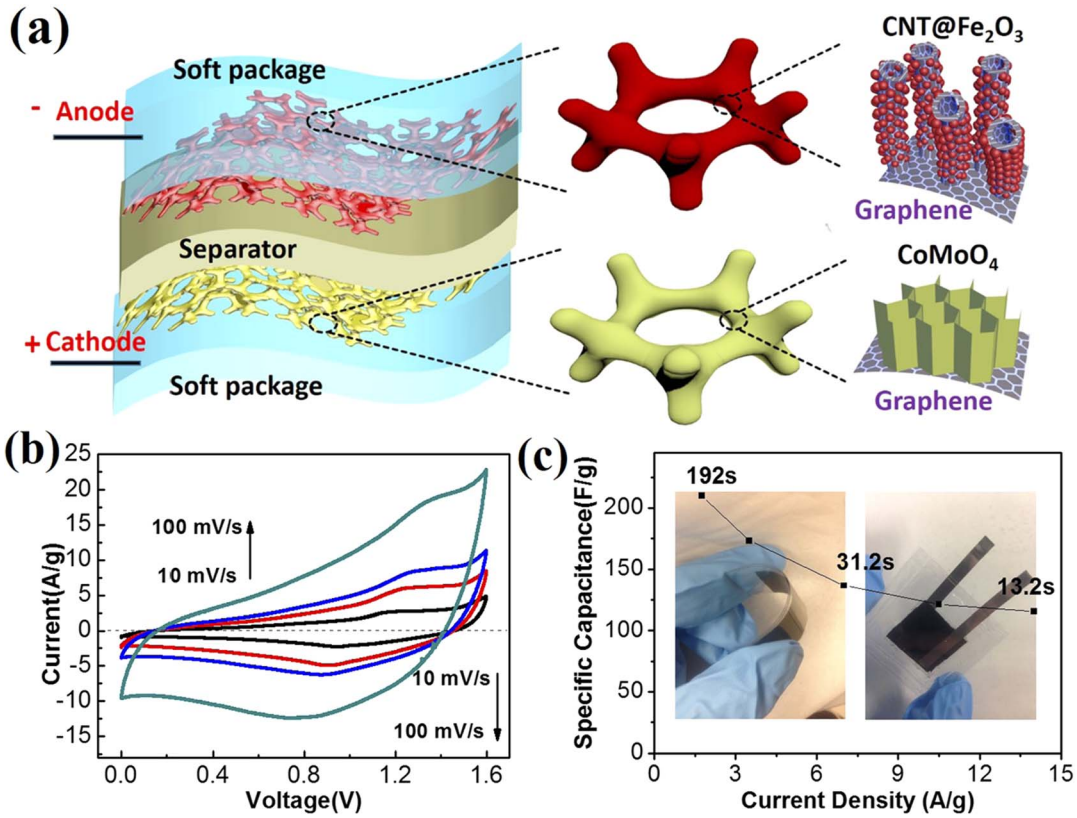

Fig. 3 Electrochemical behavior of the GF–CNT/Fe_2O_3//GF–$CoMoO_4$ full cell. (a) Schematic of the full-cell package. (b) CV curves, (c) rate capability.

Table 1 Investigating the specific capacitance of different types of composites based on carbon materials/metal oxides

Composite	Specific capacitance	Current density	Reference
$Ni(OH)_2$–MnO_2–RGO	1985 F g^{-1}	1 A g^{-1}	135
Graphene sheet/porous NiO	400 F g^{-1}	2 A g^{-1}	136
NiO/RGO	1016.6 F g^{-1}	1 A g^{-1}	137
Carbon-coated mesoporous NiO nanoparticles	931 F g^{-1}	2 A g^{-1}	138
NiO/Ni/rGO	2048.3 F g^{-1}	1 A g^{-1}	139
$Ni(OH)_2$/graphene/nickel	2161 F g^{-1}	1 A g^{-1}	140
$Ni(OH)_2$/AC/CNT	1038 F g^{-1}	1 A g^{-1}	141
α-Fe_2O_3/rGO	970 F g^{-1}	1 A g^{-1}	142
Co_3O_4 nanowire network coated on a carbon fiber	1124 F g^{-1-1}	0.25 A g^{-1}	143
Co_3O_4 nanoparticles on vertically aligned graphene nanosheets	3560 F g^{-1}	1 A g^{-1}	144
Fe_2O_3/ACC	1181 F g^{-1}	5 A g^{-1}	145
Graphene–CeO_2	110 F g^{-1}	1 A g^{-1}	146
CeO_2/MWCNTs	455.6 F g^{-1}	1 A g^{-1}	147
CeO_2/CNTs	818 F g^{-1}	1 mV s^{-1}	148
Nb_2O_5/rGO	620.5 F g^{-1}	1 mV s^{-1}	149

4.2. Nanocomposites of carbon materials/metal sulfides

Metal sulfides are another category of electroactive materials that have been extensively studied in recent years. Metal sulfides have a high specific capacitance, good energy density, and good supercapacitor properties. However, metal sulfides are oxidized in the vicinity of air, which limits the use of metal sulfides as electroactive materials in supercapacitors. As mentioned before, carbonaceous materials are an important candidate for the manufacture of nanocomposite electrode materials for improving the electrical conductivity and the specific surface area. Preparing composites based on metal sulfides and carbon materials prevents the oxidation of metal sulfides, increases the specific surface area, and improves the supercapacitor properties. Shen *et al.* used a hydrothermal method to cover nickel sulfide on carbon and then put it on to a graphene oxide sheet. Various composites with different

percentages of the precursor material were also prepared to achieve optimal electrode materials. The electrochemical behaviors of RGO and CCNS were investigated to determine the effect of each component in the composite on the final performance. The results confirmed the synergistic effect and high specific surface area. Finally, the CCNS–RGO composite showed a specific capacitance of 860.1 F g^{-1} at 5 mV s^{-1}.[150] Vickraman *et al.* synthesized nickel sulfide and carbon-based nanocomposites with a core–shell structure. In this study, to obtain stable materials, nanocomposites were prepared with different proportions of carbon and nickel sulfide. The nanocomposite with 1% carbon and 0.5% nickel sulfide confirmed the achievement of an electroactive material with good supercapacitor properties (specific capacitance of 1022 F g^{-1} at 1 A g^{-1}).[151] Using a multi-step method, Yang *et al.* first synthesized nickel oxide coated with carbon and then synthesized a nanocomposite based on nickel oxide coated with carbon with reduced graphene oxide. Finally, the nanocomposite based on nickel sulfide coated with carbon and reduced graphene oxide (Ni_3S_2–C/rGO) (Fig. 4) was synthesized by sulfonation. The stable structure of the nanocomposite confirmed the achievement of good supercapacitor properties with high conductivity.[152]

In another study, a nanocomposite based on copper-nickel sulfide and carbon nanotubes (obtained by placing copper–nickel sulfide in the structure of carbon nanotubes) was synthesized. The NiCuS/CNT composite demonstrated high stability and power density, and showed a specific capacity of 1110.0 C g^{-1}. Investigation of the performance of the nanocomposite supercapacitors in an asymmetric device revealed a power density of 52.5 W h kg^{-1} at 750 W kg^{-1}, indicating its potential as an efficient device.[153] Sreeja *et al.* synthesized a composite based on cobalt sulfide (CoS) and two other carbon materials, namely graphene oxide (rGO) and multi-walled carbon nanotubes (MWCNTs), using a hydrothermal method. Investigation of the electrochemical behavior of this nanocomposite showed there was a synergistic effect between the sulfided metal (CoS) and other carbon materials (MWCNTs and rGO). The conductivity created by the carbon materials in this nanocomposite (rGO/MWCNT/CoS) confirmed the achievement of a nanocomposite with ideal supercapacitor properties (with the quasi-capacitance behavior of metal sulfide in addition to the high conductivity of carbon materials). A specific capacity of 612 F g^{-1} was obtained at a power density of 1 A g^{-1} for the nanocomposite.[154] Raj Xavier *et al.* synthesized a carbon nanotube-based nanocomposite and two types of metal sulfides (nickel sulfide and cobalt sulfide) using a facile method. Investigation of the supercapacitor properties of the CNTs/NiS/CoS nanocomposite confirmed the low resistance of this nanocomposite. Comparing the impedance of the carbon nanotubes with the CNTs/NiS/CoS nanocomposite showed that the resistance of the CNTs/NiS/CoS nanocomposite was decreased compared to the carbon nanotubes due to the synergistic effect between the components of the nanocomposite.[155] Manganese oxide is a commonly used electrode material in supercapacitors due to its biocompatibility and cheapness. However, manganese oxide has a low specific capacitance, which has led to the use of manganese sulfide as an alternative electrode material with good supercapacitor properties. Manganese sulfide with a γ-phase (layered structure) has good supercapacitor properties because its structure provides conditions for more electrolyte ion penetration. Tang *et al.* synthesized a composite based on manganese sulfide and graphene oxide with the Kirkendall effect. The three-dimensional morphology of the MnS/GO-NH_3 composite led to its high-efficiency supercapacitor performance. According to the synthesis route shown in Fig. 5, MnS/GO-NH_3, MnS/GO, and Mn $(OH)_2$/GO electrode materials were formed in a single synthesis route. Investigation of the electrochemical behavior of all three materials showed that MnS/GO-NH_3 had higher conductivity and specific capacitance. Also, the redox peaks of the MnS/GO-NH_3 composite were reduced compared to those of the MnS/GO-NH_3 and MnS/GO electrode materials.[156]

Deng *et al.* prepared composites based on eggplant-derived carbon materials and $NiCo_2S_4$. The electrochemical results showed that the specific capacitance of the composite was 4 times higher than that of $NiCo_2S_4$. The composite synthesis ($NiCo_2S_4$–carbon derived from eggplant) was done by creating

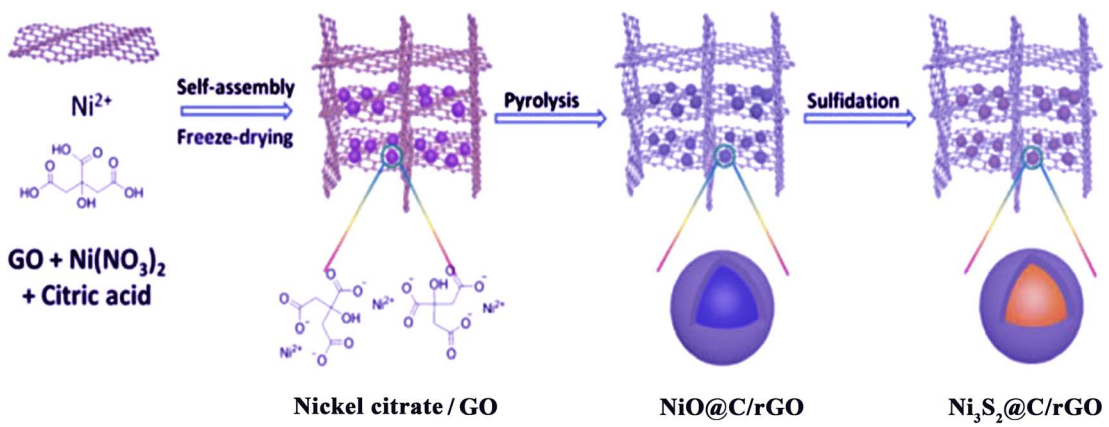

Fig. 4 Schematic of the synthesis of dual carbon-modified Ni_3S_2–C/rGO.[152]

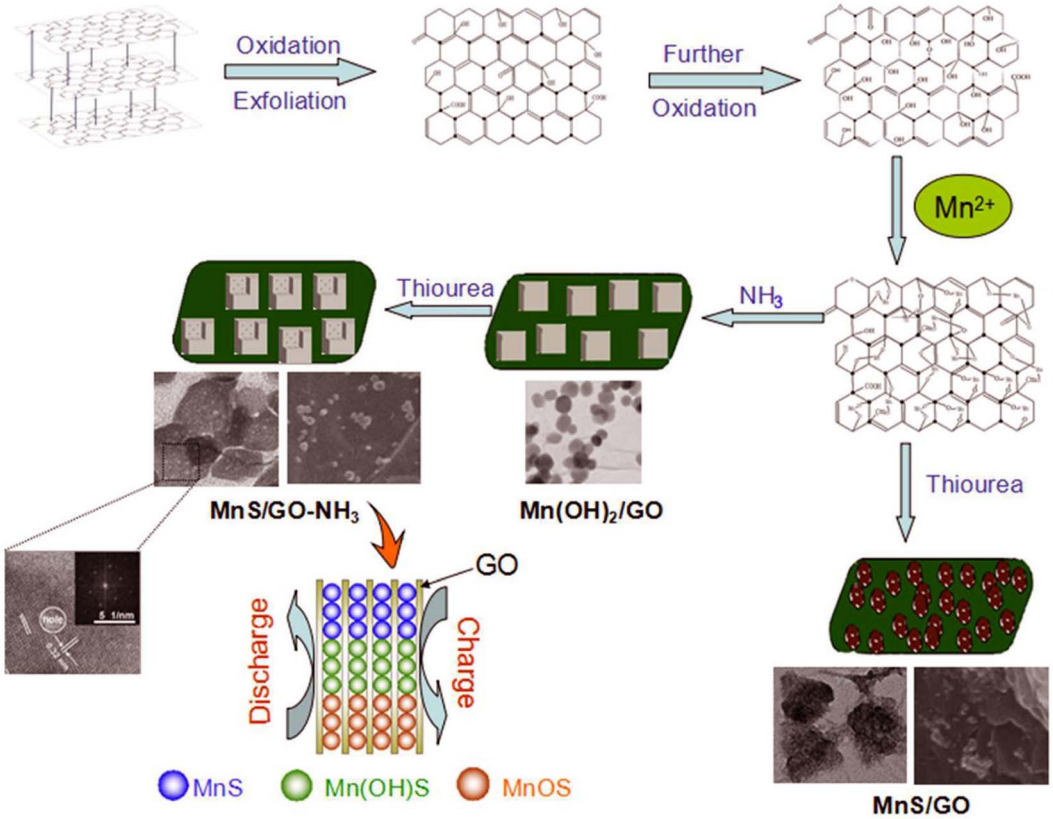

Fig. 5 Schematic of the preparation processes of MnS/GO-NH_3 and MnS/GO composites.[156]

Table 2 Investigating the specific capacitance of different types of composites based on carbon materials/metal sulfides

Composite	Specific capacitance	Current density	Reference
MWCNTs/NiS_2	2054.28 F g^{-1}	2 A g^{-1}	158
$NiCo_2S_4$@CNT	1123 F g^{-1}	0.5 A g^{-1}	159
C/$NiCo_2S_4$	1545 F g^{-1}	10 A g^{-1}	160
$NiCo_2S_4$/carbon nanotube	2210 F g^{-1}	1 A g^{-1}	161
$NiCo_2S_4$/carbon-filled nickel foam complex	9.28 F cm^{-2}	4 mA cm^{-2}	162
$NiCo_2S_4$/CNTs	1690 F g^{-1}	5 A g^{-1}	163
CoS_2/AC/g-C_3N_4	984 F g^{-1}	5 A g^{-1}	164
CoS/nitrogen-doped carbon	789 F g^{-1}	5 A g^{-1}	165
CoS_2/S, N co-doped porous carbon	306 F g^{-1}	1 A g^{-1}	166
Co_3O_4/CoS	764.2 F g^{-1}	1 A g^{-1}	167
g-CuS/Cc-SC	1333 mF cm^{-2}	2 mA cm^{-2}	168
CuS–MWCNTs	2831 F g^{-1}	1 A g^{-1}	168
CuS/CC-4	213.8 C g^{-1}	0.49 A g^{-1}	169
CuS/CNT	1960 F g^{-1}	10 mA cm^{-2}	170
CuS/MWCNT	396.7 F g^{-1}	1 A g^{-1}	171
ANPC@CuS	1112.92 F g^{-1}	1 A g^{-1}	172
CuS/carbonized cotton	4176 mF cm^{-2}	2 mA cm^{-2}	173
CuS/C-dots	2642 F g^{-1}	2 A g^{-1}	174
CuS/3DG	249 F g^{-1}	4 A g^{-1}	175
rGO/CuS	235 C g^{-1}	1 A g^{-1}	176
CuS@CQDs	920.5 F g^{-1}	0.5 A g^{-1}	177
CuS–CNTs@NF	467.02 F g^{-1}	0.5 A g^{-1}	178
CC/VAGN/CuS	342.6 mA h g^{-1}	1 A g^{-1}	179
$Cu_{1.4}S$/CC	485 F g^{-1}	0.25 A g^{-1}	180
CuS/C	719 F g^{-1}	1 A g^{-1}	181

a bond between the polar groups of carbon and the cations. The final morphology of the nanocomposite displayed a flaky structure, which made it possible to achieve an efficient supercapacitor by creating a high surface area (the high surface area was due to carbon derived from eggplant).[157] Quan *et al.* synthesized a nanocomposite based on iron oxide and reduced graphene oxide (α-Fe_2O_3/rGO) and a nanocomposite based on manganese sulfide and reduced graphene oxide (α-MnS/rGO). Then, an asymmetric device was prepared from these two nanocomposites, which showed a specific capacitance of 161.7 F g^{-1} at 1 A g^{-1} [158] (Table 2).

4.3. Nanocomposites of carbon materials/metal–organic frameworks

A metal–organic framework is a crystal structure in which organic ligands link metal ions. Due to their high porosity and the high specific surface, MOFs enable high performance for supercapacitor devices. There are different methods available for the synthesis of MOFs, and the choice of each method creates unique properties. According to the general morphology of MOFs, they show efficient performance in supercapacitor devices as electrode materials. Bimetallic MOFs work better than monometallic MOFs as electrode materials. Electrode materials based on bimetallic MOFs provide good supercapacitor properties, such as simultaneously achieving high energy density and high specific capacitance. The synthesis of composites based on carbon materials and MOFs is an effective method to overcome the limitations observed in monometallic MOFs. The synergistic effect between the MOFs and carbon materials can lead to obtaining efficient electroactive materials.[182] Kolekar *et al.* synthesized composites based on MOF–Zn and reduced graphene oxide by a hydrothermal method (Fig. 6). Electrochemical analysis of the Zn-MOF–rGO composite showed it had a specific capacitance of 205 C g^{-1} at 1 A g^{-1}.[183]

In another study, a composite prepared from graphene-like carbon (nitrogen-doped) and a MOF confirmed the synergistic effect between the carbon material and the MOF. The increase in the specific surface due to the carbon compounds and the presence of nitrogen compensated for the lack of conductivity of the MOF compound, with the composite achieving a specific capacitance of 470 F g^{-1}.[184] Rai *et al.* synthesized a nanocomposite based on a copper MOF and reduced graphene oxide. The nanocomposite electrode material displayed a high specific capacitance (366.6 F g^{-1}) and high stability, showing the beneficial synergistic effect from the copper MOF and the reduced graphene oxide.[185] An increase in conductivity caused by carbon nanotubes in composites based on MOFs and carbon nanotubes was observed by Wang *et al.*, who also reported that the synergistic effect between the nickel MOF and carbon nanotube) Ni-MOF/CNT(led to a stable electrode material with a specific capacitance of 1765 F g^{-1}.[186] The layered structure of a nanocomposite based on a MOF and carbon nanotube (MOF(Ni)/CNT) prepared by the solvothermal method enabled faster electrolyte penetration and increased electrical conductivity. The asymmetric device prepared from these electrode materials demonstrated a specific capacitance of 97 F g^{-1}.[187] A nanocomposite based on a MOF (Ni/Co-MOF–rGO) and graphene oxide was prepared using a cobalt MOF as a precursor. The synthesis of the derived MOF and the composite (Ni/Co-MOF–rGO) was performed in one step, and the composite

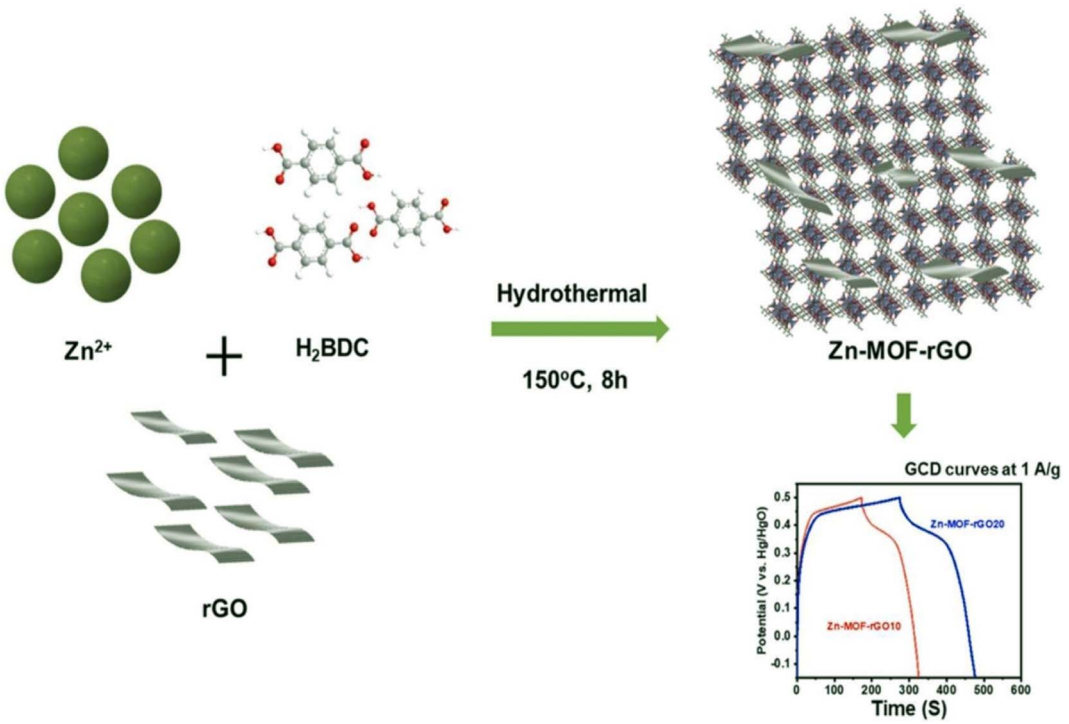

Fig. 6 Schematic of the synthesis of Zn-MOF–rGO.[183]

demonstrated a specific capacitance of 860 F g^{-1}.[188] However, traditional physical and chemical methods of preparing composites based on MOFs and carbon materials have some disadvantages. This method limits the achievement of a homogeneous composite and sometimes destroys the carbon materials. To overcome this limitation, physical green methods have been used.[189] Sulaiman *et al.* synthesized a nanocomposite based on a copper MOF and reduced graphene oxide by a hydrothermal method. Electrochemical analysis confirmed the resistance of the nanocomposite electrode materials was decreased compared to the individual components (*i.e.*, the reduced graphene oxide and MOF). These use of these electrode materials as the negative electrode in the manufacturing of asymmetric supercapacitors led to a specific capacitance of 483.9 F g^{-1}.[190]

4.3.1 MOF-derived carbon materials. Carbon materials can be obtained from MOFs, and these MOF-derived carbon materials can have unique performance properties, such as a high specific surface area, for use in energy-storage systems. However, the complex synthesis of MOFs derived from carbon materials limits their performance as electroactive materials for use in industry; in particular, the high cost and the long synthesis method limit the mass production of these materials. To overcome these limitations, Liu *et al.*[191] synthesized a MOF with cobalt ligands by a bottom-up method. The following step involved synthesis of a porous carbon structure (containing cobalt nanoparticles) by thermal decomposition of the MOF (Fig. 7).

The carbon structure with high porosity provides abundant active centers for ion transfer and increases the penetration rate of electrolyte ions.[191] The type of synthesis of the MOFs affects the final electrochemical behavior of the MOF-derived carbon materials. Mijowska *et al.* synthesized a MOF (MOF-5) derived from different carbon materials by two different methods (physical and chemical). Then, the carbon nanocomposite derived from the MOF was synthesized in the next step. The results of their electrochemical analyses showed that the nanocomposite derived from the MOF synthesized by the physical method had high stability and displayed a supercapacitor behavior.[192] A nanocomposite based on manganese oxide and carbon derived from a MOF was synthesized and its supercapacitor behavior was investigated. As can be seen in Fig. 8a, the CV curve of the MOF-derived nanocomposite in Na_2SO_4 electrolyte solution showed a pseudocapacitance behavior (apparently inductively coupled with weak redox peaks). Fig. 8b displays the charge–discharge diagram of the nanocomposite, which showed the long discharging time of the nanocomposite, indicating a supercapacitor with a high specific capacitance. Fig. 8c shows the stability of the MOF-derived nanocomposite could be maintained at 94% for up to 5000 cycles. The impedance and the fitted diagrams in Fig. 8d and e confirm the resistance and the supercapacitor behavior of the MOF-derivative nanocomposite. The Ragone plot in Fig. 8f shows the energy density was 15.5 W h kg^{-1} for the MOF-derived nanocomposite[193] (Table 3).

4.4. Nanocomposites of carbon materials/polymers

Polymers are substances of natural and synthetic origin that consist of repeating units. Among the categories related to

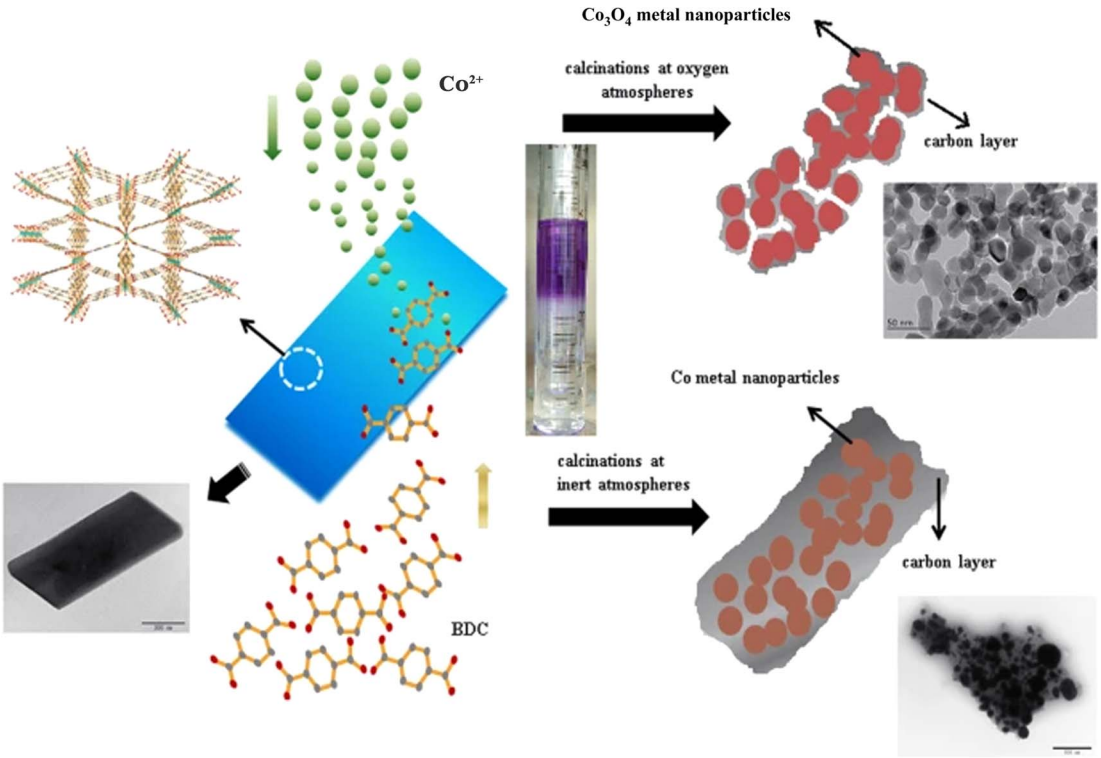

Fig. 7 Schematic of the syntheses of Co-BDC nanosheets and cobalt–carbon composites.[191]

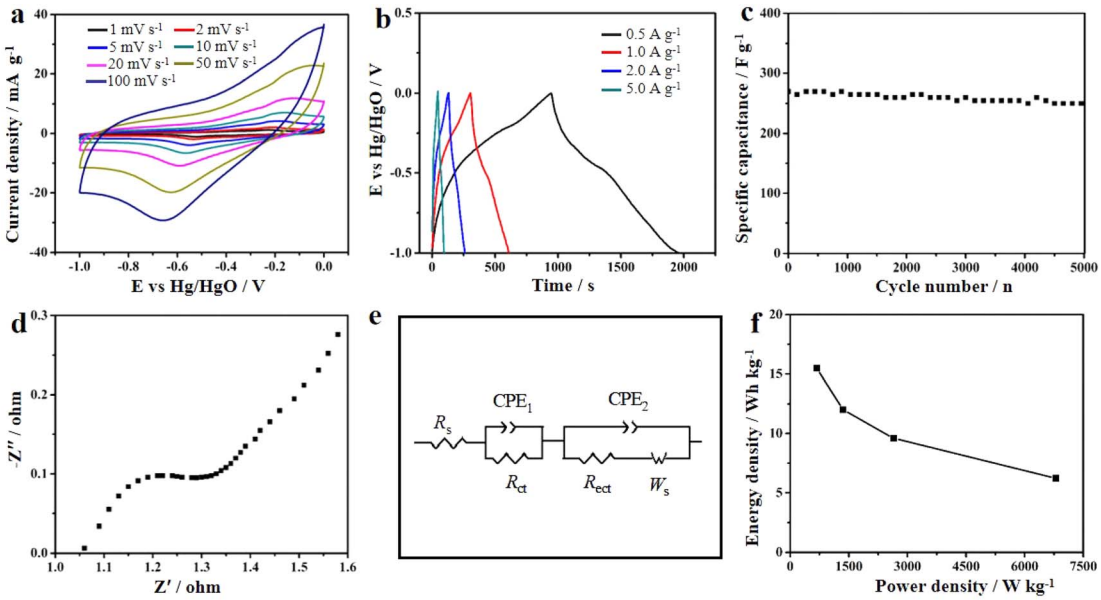

Fig. 8 Electrochemical properties of MnO/C as supercapacitors. (a) CV curves; (b) charge–discharge curves; (c) cycling stability; (d) EIS in a high-frequency region; (e) diagram of an equivalent circuit; and (f) Ragone plot of the symmetrical supercapacitor.[193]

polymers (organic, inorganic, synthetic, non-elastomer), organic polymers, as conductive polymers, have shown good performance in energy-storage devices. Conductive polymers are called organic metals (common behavior between polymers and metals) as electrode materials with better supercapacitor properties than other inorganic materials. The electrical conductivity of conductive polymers as electrode materials is not the same as the conductivity of other electrode materials (conductive and semiconducting). The conduction mechanism of conductive polymers is not similar to other electroactive

Table 3 Investigating the specific capacitance of different types of composites based on carbon materials/MOFs and MOF-derived carbon materials

Composite	Specific capacitance	Current density	Reference
Cu-MOF/rGO	867.09 F g^{-1}	1 A g^{-1}	194
MOF–CNT	166.4 F g^{-1}	1 A g^{-1}	195
rGO–$NiCo_2S_4$ MOF	972 F g^{-1}	1 A g^{-1}	196
MOF-NPC/MnO_2	120 F g^{-1}	5 A g^{-1}	197
Fe-MOF/carbon	628.5 F g^{-1}	1 A g^{-1}	198
Carbon nanosheet derived from a 2D Cu-MOF	260.5 F g^{-1}	0.5 A g^{-1}	199
MOF-derived N-doped carbon	44 F g^{-1}	0.67 A g^{-1}	200
MOF-derived hierarchical carbon network	385 F g^{-1}	0.1 A g^{-1}	201
γ-CD-MOF	283.3 F g^{-1}	1 A g^{-1}	202
Nitrogen-doped carbon-enriched MOF	2727.5 F g^{-1}	1.0 A·g^{-1}	203
G/Co-MOF-derived 3DPC/Co_3O_4	423 F g^{-1}	1 A g^{-1}	204
MOF-derived nanoporous	545 F g^{-1}	1 A g^{-1}	205
MOF-derived carbon	174 F g−1	1 A g^{-1}	206
Co-MOF/MX-CNF	475.4 mA h g^{-1}	1 A g^{-1}	207
MOF-derived phosphorus-doped porous carbons	168 F g^{-1}	1 A g^{-1}	208
MOF-derived nitrogen-doped porous carbons	230 F g^{-1}	1A g^{-1}	209
CC/CoNi-MOF	177.7 F g^{-1}	0.21 A g^{-1}	210
MOF-derived Mn_3O_4–C/rGO	382.1 F g^{-1}	1 Ag^{-1}	211
MOF-derived Co_9S_8/NS–C	734 F g^{-1}	1 Ag^{-1}	212
NiCo-MOF/MWCNT	1010 F g^{-1}	0.5 A g^{-1}	213
MOF-derived CNT/NiO	996 F g^{-1}	1 A g^{-1}	214
MOF-derived NiS_2/C	1572 F g^{-1}	0.5 A g^{-1}	215
MOF-derived Ni–CoP/C	708.1 F g^{-1}	1 A g^{-1}	216
Ni-MOF-derived NiO/C	496 C g^{-1}	1 A g^{-1}	217
MOF-67-derived C	24.7 F cm^{-2}	1 mA cm^{-2}	218

materials. In general, the conduction mechanism of conductive polymers is a combination of electrical conductivity and ionic conductivity. Therefore, conductive polymers show a double charge-transfer mechanism, and when the π–π electrons are transferred, a conductive path is created. During the electrochemical reactions performed on the surface of conductive polymers, ions move on the surface of the conductive polymer, which causes a change in the oxidation state[219] Among conductive polymers, polyaniline is among the most biocompatible and can be obtained *via* a facile synthesis method. The high conductivity, low density, and good mechanical properties of polyaniline have made polyaniline a suitable candidate for preparing nanocomposites to improve the performance of semiconductor materials. However, some nanocomposites based on polyaniline and semiconductor materials are less stable due to the swelling caused by the doping process of polyaniline chains. Therefore three-component nanocomposites based on semiconducting materials, polyaniline, and carbon materials have been synthesized to overcome this limitation. Liu *et al.* synthesized a nanocomposite based on vanadium oxide, conductive polymer, and carbon nanotubes, and the resulting nanocomposite showed an increase in stability and specific capacitance compared to those of the individual components.[220] The synergistic effect between polyaniline and carbon nanotubes and $NiMnO_3$ made it possible to achieve a supercapacitor with high stability, high power density, and a specific capacitance of 1276 F g^{-1}.[221] The synergistic effect between silver ions, activated carbon, and polyaniline enabled obtaining efficient electrode materials.[222]

A composite of MWCNTs with polyaniline synthesized by a self-dispersion method enabled obtaining electrode materials that displayed a specific capacitance of 1017 F g^{-1} due to the synergistic effect between the polyaniline and MWCNTs.[223] Composite synthesis based on carbon materials and polyaniline allowed obtaining a flexible supercapacitor that was shown to be stable under mechanical stress. The synthesis of electrode materials based on carbon nanotubes, polyaniline, and graphene was used to prepare flexible supercapacitors with desirable supercapacitor properties.[224] Chen *et al.* reported a three-component nanocomposite synthesized on carbon nanotube fibers in which the shell–shell structured N-CNTs were formed and then polyaniline was deposited on the N-CNTs. The carbon nanotube fibers increased the speed of electron transfer and improved the interaction between the other components (PANI and N-CNTs), while the N-CNTs increased the rate of ion transfer and the rate of electron transfer at the same time. The synergistic effect between the three components of the composite led to it displaying a specific capacitance of 221.3 F g^{-1}.[225] Polyaniline's cyclic stability was achieved by preparing a composite based on polyaniline and MWCNTs combined with activated carbon (A-MWCNT/PANI). The carbon materials ensured the polyaniline polymer matrix was homogeneous. In a study conducted by Park *et al.*, activated MWCNTs were used to homogenize the surface of polyaniline to improve the stable cycle. Activation of the MWCNTs increased the specific surface area of nanotubes, which had a great effect on improving the final performance of the nanocomposites. Also, the interactions created between the carbon (π-conjugated) and polyaniline (quinoid ring) components accelerated the charge-transfer process.[226] Activated carbon has been used to preserve the polyaniline polymer chain from degradation during charge–discharge cycles, which can enable obtaining stable electrode materials. In many cases, the specific capacitance of polyaniline is higher than the composite based on carbon and polyaniline materials, so the synthesis of nanocomposites based on polyaniline and carbon materials can be performed to increase the cyclic stability of electrode materials.[227] To determine the influence of the synthesis method on the final performance of electrode materials based on nanocomposites derived from carbon materials and polyaniline, a study was conducted by Morallón *et al.* comparing the synthesis of nanocomposite electrode materials obtained by two chemical and electrochemical methods. Two asymmetric devices were prepared from nanocomposites synthesized by electrochemical and chemical methods using activated carbon as the negative electrode. The supercapacitor behaviors of the asymmetric devices were investigated using H_2SO_4 electrolyte. A better supercapacitor behavior was obtained for the asymmetric device of the nanocomposite prepared by the chemical method, displaying an energy density of 20 W h kg^{-1}.[228] A flexible supercapacitor for use in wearable electronics was obtained by Chen *et al.* based on a composite prepared from activated carbon fiber, polyaniline, and carbon nanosheets. Their investigations into the electrochemical behavior of the active carbon fiber (ACFF) used in the manufacture of wearable electronics showed it had poor electrical conductivity; however, the high porosity of ACFF facilitated the absorption of electrolyte ions, so the low specific capacity of these materials corresponded to the poor electrical conductivity. To improve the performance of ACFF, different ratios of polyaniline (0.5, 0.1, 0.15, and 0.2) were combined with ACFF. CV analysis of the prepared composites confirmed the nanocomposite containing 0.1% polyaniline had higher specific capacitance. To improve the electrical conductivity of nanocomposite based on polyaniline and ACFF a three-component nanocomposite based on polyaniline, ACFF, and carbon nanotube was synthesized. The obtained nanocomposite showed a high specific capacitance of 5476 mF cm^{-2}.[229] Activated carbon derived from biomaterials has demonstrated high performance in energy-storage systems. Du *et al.* synthesized celery-derived activated carbon at 500 °C under CO_2 gas. Next, a composite based on polyaniline and celery-derived activated carbon was synthesized. Then nitrogen-doped porous carbon was synthesized by carbonization of the composite formed at 850 °C under nitrogen gas. The electrochemical behavior of the obtained nitrogen-doped porous carbon electrode material was investigated in H_2SO_4 electrolyte solution and showed a specific capacitance of 402 F g^{-1}.[230] Xie *et al.* reported synthesizing ACFs (fibers substrate of activated carbon) by a hydrothermal method under argon gas and then polyaniline was grown on the ACFs. The ACFs demonstrated increasing electrical conductivity, which led to the achievement of efficient electrode materials with a specific capacitance of 296.3 F g^{-1}.[231] Carbon materials, including activated carbon and graphene oxide, which can be added to increase the cyclic stability of polyaniline, have low

Table 4 Investigating the specific capacitance of different types of composites based on carbon materials/MOFs and polymers

Composite	Specific capacitance	Current density	Reference
Mn-CPANI	329 F g^{-1}	1 A g^{-1}	233
AC/PANI/PVA	66.6 F g^{-1}	1 A g^{-1}	234
PANI/AC	35 F g^{-1}	1 A g^{-1}	235
PANI/AC/TiO_2 nanowires	286 F g^{-1}	1 A g^{-1}	236
ACC/PANI	369 F g^{-1}	50 mA g^{-1}	237
PANI/AC/CuF	248.3 F g^{-1}	1 A g^{-1}	238
PANI/AC	549.5 F g^{-1}	1 A g^{-1}	239
PANI/AC	1250 F g^{-1}	1 A g^{-1}	240
PANI-TU-ACF	563.8 F g^{-1}	1 A g^{-1}	241
NSAC-PANI-2	304 F g^{-1}	1 A g^{-1}	242
PANI/nTiO_2/AC	827 F g^{-1}	10 mV s^{-1}	243
AC/PANI	437.9 F g^{-1}	0.5 A g^{-1}	244
PANI/GO/$CuFe_2O_4$	614.76 F g^{-1}	0.5 A g^{-1}	245
PCNT-NMP-40	917.3 F g^{-1}	1 A g^{-1}	246
AC//Pani-C	230 F g^{-1}	1 A g^{-1}	247
rGO/PANI/PB	336 F g^{-1}	1 A g^{-1}	248
PANI/CNTs	389.5 F g^{-1}	0.5 A g^{-1}	249
PANI/(TOCNF-SMWCNT)	546 F g^{-1}	1 A g^{-1}	250

solubility in water, so choosing hydrophilic carbon materials, such as carbon-based quantum dots, can be a suitable alternative. Thambusamy *et al.* synthesized quantum dots derived from ascorbic acid, with an aim to take advantage of the high electrical conductivity of ascorbic acid, by a hydrothermal method at 180 °C. Then a PANI–CQD–Cu nanocomposite was synthesized by polymerization from aniline monomer, $CuSO_4$, and CQD derived from ascorbic acid. The conductivity of the PANI was improved by the presence of the CQD surface functional groups along with the redox catalytic property of copper ions. The electrochemical behaviors of the polyaniline and polyaniline–CQD–Cu nanocomposite and polyaniline–copper and polyaniline–CQD composites were investigated in the same electrolyte (1 M H_2SO_4), with the high supercapacitor performance of the polyaniline–CQD–Cu nanocomposite demonstrated, with a specific capacitance of 1070 F g^{-1} [232] (Table 4).

4.5. Nanocomposites of carbon materials/MXenes

The first report of MXene synthesis was recorded in 2011 by Gogotsi *et al.*[251] MXenes consist of the $M_{n+1}AX_n$ phase ($n = 1, 2, 3\ldots$), where M, A, and X are transition metals, IIIA or IVA elements, and carbon or nitrogen, respectively. Despite having good physical and chemical properties as electrode materials, MXenes have low cyclic stability. The performance of MXenes as electrode material can be improved by the formation of carbon/MXene-based composites. Carbon materials increase the electrolyte diffusion rate by increasing the specific surface area, enabling obtaining electrode materials with high stability and specific capacitance. The synthesis methods of MXenes include electrostatic, hydrothermal, and solvothermal methods. Sathish *et al.* synthesized N-(Nb_2CTx/rGO) using a supercritical fluid method. Nb_2CTx synthesized by the supercritical fluid method has better supercapacitor properties than other MXenes. The electrochemical behavior of (Nb_2CTx/rGO) was investigated in H_2SO_4, $TEABF_4$/ACN, and PVA/H_2SO_4 electrolytes, and the stability of the N-(Nb_2CTx/rGO) electrode material in the PVA/H_2SO_4 electrolyte was recorded as 100% at up to 100 000 cycles. The 2D/2D structure of the N-(Nb_2CTx/rGO) composite with high specific surface area suggest its potential use as a commercial electrode material with high stability (100% stability) and provide the basis for further studies in this field.[252]

6. Conclusion

In this study, by reviewing the electrochemical properties of different types of carbon-based nanocomposites as electrode materials, the effect of each type of carbon material (CNT, AC, CQD, GO, and RGO) on improving the various types of electroactive materials (metal oxides, conductive polymers, MOFs, and metal sulfides) was investigated. The combination of carbon materials with metal oxides reduces the faradaic current while the synergistic effect between the metal oxides and carbon materials enables obtaining electrode materials with high specific capacitance. Carbon materials prevent the oxidation of metal sulfides in the vicinity of air. Composites based on carbon materials and MOFs can enable obtaining electrode materials with a larger specific surface area. Finally, carbon materials can improve the cyclic stability of conductive polymers and prevent the destruction of polymer chains during long charge–discharge cycles. This review study, by comprehensively examining the effect of carbon materials in improving the performance of other electroactive materials, provides insights for further innovative studies by researchers in this field.

Data availability

This manuscript is a review, and all data presented are sourced from cited references.

Conflicts of interest

The authors have no conflict of interest.

Acknowledgements

The authors gratefully acknowledge the University of Payame Noor and University of Economics (UNEC) for the financial support for this research.

References

1 H. Nazarpourfard, L. F. Aval and D. P. Dubal, *Mater. Adv.*, 2023, **4**, 6152–6174.
2 X. Zhang, H. Zhang, C. Li, K. Wang, X. Sun and Y. Ma, *RSC Adv.*, 2014, **4**, 45862–45884.
3 K. H. H. Aziz, F. S. Mustafa, K. M. Omer, S. Hama, R. F. Hamarawf and K. O. Rahman, *RSC Adv.*, 2023, **13**, 17595–17610.
4 M. A. Hossain, M. S. I. S. Kawsar Sheikh, K. R. Hossain, X. Yao, C. Bai and X. Wang, *Chem. Rev. Lett.*, 2023, **6**, 461–478.
5 L. Zhang, H. Guo, W. Zong, Y. Huang, J. Huang, G. He, T. Liu, J. Hofkens and F. Lai, *Energy Environ. Sci.*, 2023, **16**, 4872–4925.
6 Ș. Neațu, F. Neațu, I. M. Chirica, I. Borbáth, E. Tálas, A. Tompos, S. Somacescu, P. Osiceanu, M. A. Folgado and A. M. Chaparro, *J. Mater. Chem. A*, 2021, **9**, 17065–17128.
7 Y. Zhong, J. Liu, X. Wu, Z. Guguchia, J.-X. Yin, A. Mine, Y. Li, S. Najafzadeh, D. Das and C. Mielke III, *Nature*, 2023, **617**, 488–492.
8 S. A. Kadam, K. P. Kadam and N. R. Pradhan, *J. Mater. Chem. A*, 2024, **12**, 17992–18046.
9 F. Alimola, N. Arsalani and I. Ahadzadeh, *Mater. Chem. Phys.*, 2024, **319**, 129293.
10 A. Pramuanjaroenkij and S. Kakaç, *Int. J. Hydrogen Energy*, 2023, **48**, 9401–9425.
11 S. Kalnaus, N. J. Dudney, A. S. Westover, E. Herbert and S. Hackney, *Science*, 2023, **381**, eabg5998.
12 C. Lee, W. J. Kort-Kamp, H. Yu, D. A. Cullen, B. M. Patterson, T. A. Arman, S. Komini Babu, R. Mukundan, R. L. Borup and J. S. Spendelow, *Nat. Energy*, 2023, **8**, 685–694.
13 T. Cao, K. Huang, Y. Shi and N. Cai, *Energy Environ. Sci.*, 2017, **10**, 460–490.
14 K. I. Ozoemena, *RSC Adv.*, 2016, **6**, 89523–89550.
15 L. Fagiolari, M. Sampò, A. Lamberti, J. Amici, C. Francia, S. Bodoardo and F. Bella, *Energy Storage Mater.*, 2022, **51**, 400–434.
16 A. Ray and B. Saruhan, *Materials*, 2021, **14**, 2942.
17 S. B. Mujib, F. Ribot, C. Gervais and G. Singh, *RSC Adv.*, 2021, **11**, 35440–35454.
18 M. Yaseen, M. A. K. Khattak, M. Humayun, M. Usman, S. S. Shah, S. Bibi, B. S. U. Hasnain, S. M. Ahmad, A. Khan and N. Shah, *Energies*, 2021, **14**, 7779.
19 F. Alimola, N. Arsalani and I. Ahadzadeh, *Electrochim. Acta*, 2022, **417**, 140283.
20 A. G. Olabi, Q. Abbas, A. Al Makky and M. A. Abdelkareem, *Energy*, 2022, **248**, 123617.
21 Y. Yang, Y. Han, W. Jiang, Y. Zhang, Y. Xu and A. M. Ahmed, *Appl. Sci.*, 2021, **12**, 354.
22 Y. Li, T. Liu, Y. Liu, F. Meng and Z. Cao, *Chem. Eng. J.*, 2024, **479**, 147906.
23 T. L. Kulova, V. N. Fateev, E. A. Seregina and A. S. Grigoriev, *Int. J. Electrochem. Sci.*, 2020, **15**, 7242–7259.
24 H. Xu and M. Shen, *Int. J. Energy Res.*, 2021, **45**, 20524–20544.
25 H. Shayeghi, F. Monfaredi, A. Dejamkhooy, M. Shafie-Khah and J. Catalão, *Int. J. Electr. Power Energy Syst.*, 2021, **125**, 106391.
26 N. Arya, Y. Chandran, B. Luhar, P. Kajal, S. Powar and V. Balakrishnan, *ACS Appl. Mater. Interfaces*, 2023, **15**, 34818–34828.
27 J. Cherusseri, D. Pandey and J. Thomas, *Batteries Supercaps*, 2020, **3**, 860–875.
28 A. Abdellah, D. Toumi and S. Moreau, *Adv. Electr. Electron. Eng.*, 2022, **20**, 154–169.
29 P. Forouzandeh, V. Kumaravel and S. C. Pillai, *Catalysts*, 2020, **10**, 969.
30 S. Veeresh, H. Ganesha, Y. Nagaraju, H. Vijeth, M. Vandana, M. Basappa and H. Devendrappa, *J. Energy Storage*, 2022, **52**, 104715.
31 X. Chen, Q. Liu, T. Bai, W. Wang, F. He and M. Ye, *Chem. Eng. J.*, 2021, **409**, 127237.
32 D. J. Ahirrao, A. K. Pal, V. Singh and N. Jha, *J. Mater. Sci. Technol.*, 2021, **88**, 168–182.
33 M. Vandana, S. Veeresh, H. Ganesh, Y. Nagaraju, H. Vijeth, M. Basappa and H. Devendrappa, *J. Energy Storage*, 2022, **46**, 103904.
34 M. Shaheen, M. Z. Iqbal, M. W. Khan, S. Siddique, S. Aftab and S. M. Wabaidur, *Energy Fuels*, 2023, **37**, 4000–4009.
35 K. Wang, Z. Wang, J. Liu, C. Li, F. Mao, H. Wu and Q. Zhang, *ACS Appl. Mater. Interfaces*, 2020, **12**, 47482–47489.
36 X. Shi, L. Sun, X. Li, L. Wu, J. Qian, J. Wang, Y. Lin, S. Su, C. Sun and Y. Zhang, *J. Colloid Interface Sci.*, 2022, **606**, 135–147.
37 C. Hu, L. Miao, Q. Yang, X. Yu, L. Song, Y. Zheng, C. Wang, L. Li, L. Zhu and X. Cao, *Chem. Eng. J.*, 2021, **410**, 128317.
38 P. Avasthi, N. Arya, M. Singh and V. Balakrishnan, *Nanotechnology*, 2020, **31**, 435402.
39 R. Mohammadi, *Chem. Rev. Lett.*, 2022, **5**, 133–140.
40 R. Bian, D. Song, W. Si, T. Zhang, Y. Zhang, P. Lu, F. Hou and J. Liang, *ChemElectroChem*, 2020, **7**, 3663–3669.
41 C. Zhang, Q. Wang, W. Zhang, X. Li, Z. Zhu, C. Zhang, A. Xie and S. Luo, *Ionics*, 2021, **27**, 3543–3551.
42 J. Ben, Z. Song, X. Liu, W. Lü and X. Li, *Nanoscale Res. Lett.*, 2020, **15**, 1–8.
43 Y. Jiang, J. Ou, Z. Luo, Y. Chen, Z. Wu, H. Wu, X. Fu, S. Luo and Y. Huang, *Small*, 2022, **18**, 2201377.
44 J. Dai, Y. Lv, J. Zhang, D. Zhang, H. Xie, C. Guo, A. Zhu, Y. Xu, M. Fan and C. Yuan, *J. Colloid Interface Sci.*, 2021, **590**, 591–600.
45 N. I. Jalal, R. I. Ibrahim and M. K. Oudah, *J. Phys.:Conf. Ser.*, 2021, **1973**, 012015.
46 R. Taslim, A. Apriwandi and E. Taer, *ACS Omega*, 2022, **7**, 36489–36502.
47 M. Gaire, B. Subedi, S. Adireddy and D. Chrisey, *RSC Adv.*, 2020, **10**, 40234–40243.

48 V. Kushwaha, A. Gupta, R. B. Choudhary, K. Mandal, R. Mondal and P. Singh, *Phys. Chem. Chem. Phys.*, 2023, **25**, 555–569.
49 J. Sun, B. Luo and H. Li, *Adv. Energy Sustainability Res.*, 2022, **3**, 2100191.
50 M. Brza, S. Aziz, H. Anuar and F. Ali, *Polym. Test.*, 2020, **91**, 106813.
51 S. B. Aziz, M. Hamsan, M. Brza, M. Kadir, S. Muzakir and R. T. Abdulwahid, *J. Mater. Res. Technol.*, 2020, **9**, 8355–8366.
52 A. S. Asnawi, S. B. Aziz, M. M. Nofal, M. H. Hamsan, M. A. Brza, Y. M. Yusof, R. T. Abdilwahid, S. K. Muzakir and M. F. Kadir, *Polymers*, 2020, **12**, 1433.
53 W. Zhou, Z. Liu, W. Chen, X. Sun, M. Luo, X. Zhang, C. Li, Y. An, S. Song and K. Wang, *Batteries*, 2023, **9**, 128.
54 L. L. Zhang and X. Zhao, *Chem. Soc. Rev.*, 2009, **38**, 2520–2531.
55 W. Raza, F. Ali, N. Raza, Y. Luo, K.-H. Kim, J. Yang, S. Kumar, A. Mehmood and E. E. Kwon, *Nano Energy*, 2018, **52**, 441–473.
56 N. R. Chodankar, H. D. Pham, A. K. Nanjundan, J. F. Fernando, K. Jayaramulu, D. Golberg, Y. K. Han and D. P. Dubal, *Small*, 2020, **16**, 2002806.
57 T. Brezesinski, J. Wang, S. H. Tolbert and B. Dunn, *Nat. Mater.*, 2010, **9**, 146–151.
58 L. Wang, L. Gao, J. Wang and Y. Shen, *J. Mater. Sci.*, 2019, **54**, 13685–13693.
59 Y. Shao, M. F. El-Kady, J. Sun, Y. Li, Q. Zhang, M. Zhu, H. Wang, B. Dunn and R. B. Kaner, *Chem. Rev.*, 2018, **118**, 9233–9280.
60 A. Muzaffar, M. B. Ahamed, K. Deshmukh and J. Thirumalai, *Renewable Sustainable Energy Rev.*, 2019, **101**, 123–145.
61 A. Afif, S. M. Rahman, A. T. Azad, J. Zaini, M. A. Islan and A. K. Azad, *J. Energy Storage*, 2019, **25**, 100852.
62 S. Ratha and A. K. Samantara, *Supercapacitor: Instrumentation, Measurement and Performance Evaluation Techniques*, Springer, 2018.
63 Y. Zhang, Y. Liu, Y. Bai, Y. Liu and E. Xie, *RSC Adv.*, 2020, **10**, 35295–35301.
64 N. Kularatna, K. Subasinghage, K. Gunawardane, D. Jayananda and T. Ariyarathna, *Electronics*, 2021, **10**, 1697.
65 S. Yadav and A. Sharma, *J. Energy Storage*, 2021, **44**, 103295.
66 F. Alimola, N. Arsalani and I. Ahadzadeh, *J. Alloys Compd.*, 2023, **949**, 169851.
67 K. Sharma, A. Arora and S. K. Tripathi, *J. Energy Storage*, 2019, **21**, 801–825.
68 L. Zeng, T. Wu, T. Ye, T. Mo, R. Qiao and G. Feng, *Nat. Comput. Sci.*, 2021, **1**, 725–731.
69 M. Gaire, K. Liang, S. Luo, B. Subedi, S. Adireddy, K. Schroder, S. Farnsworth and D. B. Chrisey, *RSC Adv.*, 2020, **10**, 16817–16825.
70 A. Fernandez, E. Perigo and R. Faria, *J. Energy Storage*, 2022, **51**, 104471.
71 C. Zheng, C. Cao, Z. Ali and J. Hou, *J. Mater. Chem. A*, 2014, **2**, 16467–16473.
72 R. Srinivasan, E. Elaiyappillai, E. J. Nixon, I. S. Lydia and P. M. Johnson, *Inorg. Chim. Acta*, 2020, **502**, 119393.
73 N. I. Jalal, R. I. Ibrahim and M. K. Oudah, *J. Phys.:Conf. Ser.*, 2021, **1973**, 012015.
74 R. Ahmad, U. A. Khan, N. Iqbal and T. Noor, *RSC Adv.*, 2020, **10**, 43733–43750.
75 R. Aslani and H. Namazi, *J. Ind. Eng. Chem.*, 2022, **112**, 335–347.
76 S. Iijima, *J. Cryst. Growth*, 1980, **50**, 675–683.
77 S. Kaur, A. Krishnan and S. Chakraborty, *J. Energy Storage*, 2023, **71**, 107928.
78 J. Xiao, G. Ouyang, P. Liu, C. Wang and G. Yang, *Nano Lett.*, 2014, **14**, 3645–3652.
79 D. M. Anjos, J. K. McDonough, E. Perre, G. M. Brown, S. H. Overbury, Y. Gogotsi and V. Presser, *Nano Energy*, 2013, **2**, 702–712.
80 J. K. McDonough and Y. Gogotsi, *Electrochem. Soc. Interface*, 2013, **22**, 61.
81 E.-S. V. Zran, A. Y. Yobouet, L. Kouakou, P. Marie-Sandrine, A. Trokourey and B. K. Yao, *Chem. Rev. Lett.*, 2022, **5**, 178–186.
82 H. Kone, I. A. Goure Bi, J. Ano, Y. Soro, G. H. Briton Bi and B. K. Yao, *Chem. Rev. Lett.*, 2021, **4**, 221–231.
83 B. Li, F. Dai, Q. Xiao, L. Yang, J. Shen, C. Zhang and M. Cai, *Energy Environ. Sci.*, 2016, **9**, 102–106.
84 F. Cheng, X. Yang, S. Zhang and W. Lu, *J. Power Sources*, 2020, **450**, 227678.
85 T. Chaiwon, P. Jannoey and D. A. D. Channei, *Key Eng. Mater.*, 2017, **751**, 671–676.
86 S. D. Magar, C. Leibing, J. L. Gómez-Urbano, R. Cid, D. Carriazo and A. Balducci, *Electrochim. Acta*, 2023, **446**, 142104.
87 K. Hina, H. Zou, W. Qian, D. Zuo and C. Yi, *Cellulose*, 2018, **25**, 607–617.
88 F. Jerez, P. B. Ramos, V. E. Córdoba, M. F. Ponce, G. G. Acosta and M. A. Bavio, *J. Environ. Manage.*, 2023, **330**, 117158.
89 B. Pant, G. P. Ojha, J. Acharya and M. Park, *Diamond Relat. Mater.*, 2023, **136**, 110040.
90 S. J. Rajasekaran, A. N. Grace, G. Jacob, A. Alodhayb, S. Pandiaraj and V. Raghavan, *Catalysts*, 2023, **13**, 286.
91 S. Wang, F. Chen, G. Zhuang, K. Wei, T. Chen, X. Zhang, C. Chen and P. Du, *Nano Res.*, 2023, **16**, 10342–10347.
92 V. N. Popov, *Mater. Sci. Eng., R*, 2004, **43**, 61–102.
93 B. Ghanavati, A. Bozorgian and J. Ghanavati, *Chem. Rev. Lett.*, 2022, **5**, 68–75.
94 M. F. De Volder, S. H. Tawfick, R. H. Baughman and A. J. Hart, *science*, 2013, **339**, 535–539.
95 A. Rashak and F. F. Karam, *Chem. Rev. Lett.*, 2024, **7**(8), 719–730.
96 J. Hu, G. Sang, N. Zeng, C. Lv and C. Xu, *Sens. Actuators, B*, 2022, **356**, 131344.
97 K. Setiyawan, B. Sugiantoro and N. R. Prabowo, *Mater. Sci. Forum*, 2021, **1029**, 65–72.
98 T. Hiraoka, T. Yamada, K. Hata, D. N. Futaba, H. Kurachi, S. Uemura, M. Yumura and S. Iijima, *J. Am. Chem. Soc.*, 2006, **128**, 13338–13339.

99 Y. Zhang, J. Wu, S. Zhang, N. Shang, X. Zhao, S. M. Alshehri, T. Ahamad, Y. Yamauchi, X. Xu and Y. Bando, *Nano Energy*, 2022, **97**, 107146.
100 R. Shoukat and M. I. Khan, *Microsyst. Technol.*, 2021, 1–10.
101 S. Rathinavel, K. Priyadharshini and D. Panda, *Mater. Sci. Eng., B*, 2021, **268**, 115095.
102 M. Kamel, A. Morsali, H. Raissi and K. Mohammadifard, *Chem. Rev. Lett.*, 2020, **3**, 23–37.
103 R. A. Ismail, M. H. Mohsin, A. K. Ali, K. I. Hassoon and S. Erten-Ela, *Phys. E*, 2020, **119**, 113997.
104 A. Aabir, M. Y. Naz and S. Shukrullah, in *Emerging Developments and Applications of Low Temperature Plasma*, IGI Global, 2022, pp. 85–102.
105 L. Hernandez-Tabares, J. G. Darias-Gonzalez, F. J. Chao-Mujica, L. M. Ledo-Pereda, M. Antuch, E. Carrillo-Barroso, J. E. Chong-Quero, E. Reguera and L. F. Desdin-Garcia, *J. Nanomater.*, 2021, **2021**, 6550809.
106 Y. Liu, J. He, N. Zhang, W. Zhang, Y. Zhou and K. Huang, *J. Mater. Sci.*, 2021, **56**, 12559–12583.
107 M. Saeed, Y. Alshammari, S. A. Majeed and E. Al-Nasrallah, *Molecules*, 2020, **25**, 3856.
108 K. Yang, M. Luo, D. Zhang, C. Liu, Z. Li, L. Wang, W. Chen and X. Zhou, *Chem. Eng. J.*, 2022, **427**, 132002.
109 S. Huang, X. Du, X. Li, M. Ma and L. Xiong, *Adv. Funct. Mater.*, 2021, **31**, 2104531.
110 C. Querne, T. Vignal, M. Pinault, P. Banet, M. Mayne-L'Hermite and P.-H. Aubert, *J. Power Sources*, 2023, **553**, 232258.
111 G. Sun, H. Ren, Z. Shi, L. Zhang, Z. Wang, K. Zhan, Y. Yan, J. Yang and B. Zhao, *J. Colloid Interface Sci.*, 2021, **588**, 847–856.
112 A. Abdollahi, A. Abnavi, F. Ghasemi, S. Ghasemi, Z. Sanaee and S. Mohajerzadeh, *Electrochim. Acta*, 2021, **390**, 138826.
113 B. Dousti, Y. I. Choi, S. F. Cogan and G. S. Lee, *ACS Appl. Mater. Interfaces*, 2020, **12**, 50011–50023.
114 T. De Silva, C. Damery, R. Alkhaldi, R. Karunanithy, D. H. Gallaba, P. D. Patil, M. Wasala, P. Sivakumar, A. Migone and S. Talapatra, *ACS Appl. Mater. Interfaces*, 2021, **13**, 56004–56013.
115 L. Wang, H. Yao, F. Chi, J. Yan, H. Cheng, Y. Li, L. Jiang and L. Qu, *ACS Nano*, 2022, **16**, 12813–12821.
116 N. B. Mohamed, M. F. El-Kady and R. B. Kaner, *Adv. Funct. Mater.*, 2022, **32**, 2203101.
117 Y. B. Tan and J.-M. Lee, *J. Mater. Chem. A*, 2013, **1**, 14814–14843.
118 W. Yang, M. Ni, X. Ren, Y. Tian, N. Li, Y. Su and X. Zhang, *Curr. Opin. Colloid Interface Sci.*, 2015, **20**, 416–428.
119 R. Lakra, R. Kumar, P. K. Sahoo, D. Thatoi and A. Soam, *Inorg. Chem. Commun.*, 2021, **133**, 108929.
120 H. Yang, S. Kannappan, A. S. Pandian, J.-H. Jang, Y. S. Lee and W. Lu, *Nanotechnology*, 2017, **28**, 445401.
121 S. Korkmaz and İ. A. Kariper, *J. Energy Storage*, 2020, **27**, 101038.
122 D. C. Marcano, D. V. Kosynkin, J. M. Berlin, A. Sinitskii, Z. Sun, A. Slesarev, L. B. Alemany, W. Lu and J. M. Tour, *ACS Nano*, 2010, **4**, 4806–4814.
123 A. M. Dimiev and J. M. Tour, *ACS Nano*, 2014, **8**, 3060–3068.
124 W. Yu, L. Sisi, Y. Haiyan and L. Jie, *RSC Adv.*, 2020, **10**, 15328–15345.
125 J. Song, X. Wang and C.-T. Chang, *J. Nanomater.*, 2014, **2014**, 276143.
126 S. C. Ray, *Applications of Graphene and Graphene-Oxide Based Nanomaterials*, 2015, vol. 6, pp. 39–55.
127 R. Aslani and H. Namazi, *Int. J. Pharm.*, 2023, **636**, 122804.
128 K. Ponnarasi, P. Elangovan and S. Surender, *Results Chem.*, 2024, **7**, 101355.
129 A. Subagio, A. Darari, I. S. Hakim, P. Priyono, P. Pardoyo and A. Subhan, 2018.
130 M. S. Vidhi, A. K. Singh and O. Thakur, *Ionics*, 2024, 1–13.
131 J. Sudarto, A. Subagio and R. Yudianti, *Makara J. Sci.*, 2017, **21**, 1.
132 C. H. Kim and B.-H. Kim, *J. Power Sources*, 2015, **274**, 512–520.
133 Y. Ouyang, R. Huang, X. Xia, H. Ye, X. Jiao, L. Wang, W. Lei and Q. Hao, *Chem. Eng. J.*, 2019, **355**, 416–427.
134 C. Guan, J. Liu, Y. Wang, L. Mao, Z. Fan, Z. Shen, H. Zhang and J. Wang, *ACS Nano*, 2015, **9**, 5198–5207.
135 H. Chen, S. Zhou and L. Wu, *ACS Appl. Mater. Interfaces*, 2014, **6**, 8621–8630.
136 X. Xia, J. Tu, Y. Mai, R. Chen, X. Wang, C. Gu and X. Zhao, *Chem.–Eur. J.*, 2011, **17**, 10898–10905.
137 P. Cao, L. Wang, Y. Xu, Y. Fu and X. Ma, *Electrochim. Acta*, 2015, **157**, 359–368.
138 K. Xu, R. Zou, W. Li, Q. Liu, T. Wang, J. Yang, Z. Chen and J. Hu, *New J. Chem.*, 2013, **37**, 4031–4036.
139 F. Liu, X. Wang, J. Hao, S. Han, J. Lian and Q. Jiang, *Sci. Rep.*, 2017, **7**, 17709.
140 L. Wang, X. Li, T. Guo, X. Yan and B. K. Tay, *Int. J. Hydrogen Energy*, 2014, **39**, 7876–7884.
141 L. Sui, S. Tang, Y. Chen, Z. Dai, H. Huangfu, Z. Zhu, X. Qin, Y. Deng and G. M. Haarberg, *Electrochim. Acta*, 2015, **182**, 1159–1165.
142 L. Chen, D. Liu and P. Yang, *RSC Adv.*, 2019, **9**, 12793–12800.
143 L. Yang, S. Cheng, Y. Ding, X. Zhu, Z. L. Wang and M. Liu, *Nano Lett.*, 2012, **12**, 321–325.
144 Q. Liao, N. Li, S. Jin, G. Yang and C. Wang, *ACS Nano*, 2015, **9**, 5310–5317.
145 J. Li, Y. Wang, W. Xu, Y. Wang, B. Zhang, S. Luo, X. Zhou, C. Zhang, X. Gu and C. Hu, *Nano Energy*, 2019, **57**, 379–387.
146 T. Saravanan, M. Shanmugam, P. Anandan, M. Azhagurajan, K. Pazhanivel, M. Arivanandhan, Y. Hayakawa and R. Jayavel, *Dalton Trans.*, 2015, **44**, 9901–9908.
147 D. Deng, N. Chen, Y. Li, X. Xing, X. Liu, X. Xiao and Y. Wang, *Phys. E*, 2017, **86**, 284–291.
148 Y. Luo, T. Yang, Q. Zhao and M. Zhang, *J. Alloys Compd.*, 2017, **729**, 64–70.
149 L. Kong, C. Zhang, J. Wang, W. Qiao, L. Ling and D. Long, *ACS Nano*, 2015, **9**, 11200–11208.
150 L. Ma, X. Shen, Z. Ji, S. Wang, H. Zhou and G. Zhu, *Electrochim. Acta*, 2014, **146**, 525–532.
151 A. S. Justin, P. Vickraman and B. J. Reddy, *Curr. Appl. Phys.*, 2019, **19**, 295–302.

152 J. He, C. Guo, S. Zhou, Y. Zhao, Q. Wang, S. Yang, J. Yang and Q. Wang, *Inorg. Chem. Front.*, 2019, **6**, 226–232.
153 R. Khan, M. Imran, A. M. Afzal, M. W. Iqbal, S. Mumtaz, S. A. Munnaf, M. S. Islam, R. Sajad, N. Muzaffar and M. Yaqoob, *ECS J. Solid State Sci. Technol.*, 2023, **12**, 101005.
154 N. James, S. Simon and P. Sreeja, *Mater. Today: Proc.*, 2023, in presss.
155 J. R. Xavier, S. Vinodhini and S. S. Chandraraj, *J. Cluster Sci.*, 2023, **34**, 1805–1817.
156 Y. Tang, T. Chen, S. Yu, Y. Qiao, S. Mu, J. Hu and F. Gao, *J. Mater. Chem. A*, 2015, **3**, 12913–12919.
157 Y. Liu, Z. Li, L. Yao, S. Chen, P. Zhang and L. Deng, *Chem. Eng. J.*, 2019, **366**, 550–559.
158 J. Meng, Y. Wang, X. Xie and H. Quan, *Ionics*, 2019, **25**, 4925–4933.
159 M. Yao, X. Ji, X. Ou, P. Wu and S. Cheng, *J. Power Sources*, 2022, **543**, 231829.
160 W. Lu, M. Yang, X. Jiang, Y. Yu, X. Liu and Y. Xing, *Chem. Eng. J.*, 2020, **382**, 122943.
161 Y. Lu, Z. Zhang, X. Liu, W. Wang, T. Peng, P. Guo, H. Sun, H. Yan and Y. Luo, *CrystEngComm*, 2016, **18**, 7696–7706.
162 S. Hui, T. Ju, X. Lin, Y. Li, Y. Wang and Z. Ying, *Dalton Trans.*, 2020, **49**, 12345–12353.
163 Y. Ren, X. Zhou and Z. Liu, *J. Mol. Eng. Mater.*, 2019, **7**, 1950004.
164 S. Sathish, T. A. Kumaravelu, C.-J. Yang, R. R. Jayapalan, R. Nirmala, C.-L. Dong, B.-H. Lin and R. Navamathavan, *J. Alloys Compd.*, 2024, **985**, 174076.
165 X. Wang, W. Li, Y. Xue, J. Liu, Y. Yue, C. Zhou, K. Zhu, D. Cao, Y. Chen and G. Wang, *J. Energy Storage*, 2022, **50**, 104220.
166 S. Liu, D. Gao, J. Li, K. San Hui, Y. Yin, K. N. Hui and S. C. Jun, *J. Mater. Chem. A*, 2019, **7**, 26618–26630.
167 J. Ning, T. Zhang, Y. He, C. Jia, P. Saha and Q. Cheng, *Materials*, 2017, **10**, 608.
168 K. Jin, M. Zhou, H. Zhao, S. Zhai, F. Ge, Y. Zhao and Z. Cai, *Electrochim. Acta*, 2019, **295**, 668–676.
169 W. Zhou, J. Miao, X. Yan, Y. Li, Y. Zhu, W. Zhang, M. Zhang, W. Zhu, M. S. Javed and J. Pan, *J. Electroanal. Chem.*, 2021, **897**, 115610.
170 Y. Lu, X. Liu, W. Wang, J. Cheng, H. Yan, C. Tang, J.-K. Kim and Y. Luo, *Sci. Rep.*, 2015, **5**, 16584.
171 Y. J. Yang, *Fullerenes, Nanotubes Carbon Nanostruct.*, 2017, **25**, 497–503.
172 C. Wang, S. Wei, Q. Zhu, X. Yang, B. Zhou, Z. Duan, Z. Xie and Y. Hu, *J. Energy Storage*, 2024, **91**, 112021.
173 S. Zhai, K. Jin, M. Zhou, Z. Fan, H. Zhao, Y. Zhao, X. Li and Z. Cai, *Colloids Surf., A*, 2019, **575**, 75–83.
174 I. Sarasamreen, S. Shajahan, S. A. Kumar, M. A. Haija, R. Ramesh and P. Anbarasan, *Diamond Relat. Mater.*, 2023, **140**, 110453.
175 Z. Tian, H. Dou, B. Zhang, W. Fan and X. Wang, *Electrochim. Acta*, 2017, **237**, 109–118.
176 S. I. El-Hout, S. G. Mohamed, A. Gaber, S. Y. Attia, A. Shawky and S. M. El-Sheikh, *J. Energy Storage*, 2021, **34**, 102001.
177 Y. Quan, G. Wang, L. Lu, Z. Wang, H. Xu, S. Liu and D. Wang, *Electrochim. Acta*, 2020, **353**, 136606.
178 Y. Quan, M. Zhang, G. Wang, L. Lu, Z. Wang, H. Xu, S. Liu and Q. Min, *New J. Chem.*, 2019, **43**, 10906–10914.
179 Y. Zhang, X. Cao, G. Zhuang and X. Chen, *J. Electroanal. Chem.*, 2023, **928**, 117033.
180 X. He, X. Mao, C. Zhang, W. Yang, Y. Zhou, Y. Yang and J. Xu, *J. Mater. Sci.: Mater. Electron.*, 2020, **31**, 2145–2152.
181 Z. Shuangsheng, Y. Zongrong, Y. Jiajia and F. Chuan, *CIESC J.*, 2016, **67**, 4892.
182 M. N. Khan and C. Jeong, *J. Alloys Compd.*, 2024, 176007.
183 Q. V. Thi, S. A. Patil, P. K. Katkar, I. Rabani, A. S. Patil, J. Ryu, G. Kolekar, N. T. Tung and D. Sohn, *Synth. Met.*, 2022, **290**, 117155.
184 W. Feng, C. Liu, Z. Liu and H. Pang, *Chin. Chem. Lett.*, 2024, 109552.
185 M. K. Singh, A. K. Gupta, S. Krishnan, N. Guha, S. Marimuthu and D. K. Rai, *J. Energy Storage*, 2021, **43**, 103301.
186 P. Wen, P. Gong, J. Sun, J. Wang and S. Yang, *J. Mater. Chem. A*, 2015, **3**, 13874–13883.
187 S. Sun, Y. Wang, L. Chen, M. Chu, Y. Dong, D. Liu, P. Liu, D. Qu, J. Duan and X. Li, *Colloids Surf., A*, 2022, **643**, 128802.
188 M. S. Rahmanifar, H. Hesari, A. Noori, M. Y. Masoomi, A. Morsali and M. F. Mousavi, *Electrochim. Acta*, 2018, **275**, 76–86.
189 Y. Zhang, Q. Xie, R. Shao, J. Ding, J. Liu, W. Xu and Y. Wang, *J. Energy Storage*, 2024, **86**, 111156.
190 D. Mohanadas, M. A. A. M. Abdah, N. H. N. Azman, J. Abdullah and Y. Sulaiman, *Int. J. Hydrogen Energy*, 2021, **46**, 35385–35396.
191 E. Dai, J. Xu, J. Qiu, S. Liu, P. Chen and Y. Liu, *Sci. Rep.*, 2017, **7**, 12588.
192 W. Kukulka, K. Cendrowski and E. Mijowska, *Electrochim. Acta*, 2019, **307**, 582–594.
193 Y. Qiao, N. Li, M. Dong, P. Jia, C. Ma, T. Zhang and T. Jiao, *Nanomaterials*, 2022, **12**, 4257.
194 S. Krishnan, A. K. Gupta, M. K. Singh, N. Guha and D. K. Rai, *Chem. Eng. J.*, 2022, **435**, 135042.
195 A. H. Anwer, M. Z. Ansari, F. Mashkoor, S. Zhu, M. Shoeb and C. Jeong, *J. Alloys Compd.*, 2023, **955**, 170038.
196 S. Kumar, S. Sekar, A. K. Kaliamurthy and S. Lee, *J. Mater. Res. Technol.*, 2021, **12**, 2489–2501.
197 M. Yao, X. Zhao, L. Jin, F. Zhao, J. Zhang, J. Dong and Q. Zhang, *Chem. Eng. J.*, 2017, **322**, 582–589.
198 B. Ramasubramanian, C. Chinglenthoiba, X. Huiqing, N. Xiping, H. K. Hui, S. Valiyaveettil, S. Ramakrishna and V. Chellappan, *Surf. Interfaces*, 2022, **34**, 102397.
199 Z.-X. Li, B.-L. Yang, K.-Y. Zou, L. Kong, M.-L. Yue and H.-H. Duan, *Carbon*, 2019, **144**, 540–548.
200 Z. Tang, G. Zhang, H. Zhang, L. Wang, H. Shi, D. Wei and H. Duan, *Energy Storage Mater.*, 2018, **10**, 75–84.
201 J. Pokharel, A. Gurung, A. Baniya, W. He, K. Chen, R. Pathak, B. S. Lamsal, N. Ghimire and Y. Zhou, *Electrochim. Acta*, 2021, **394**, 139058.
202 W. Xu, L.-H. Wang, Y. Chen and Y. Liu, *Mater. Today Chem.*, 2022, **24**, 100896.
203 D. Huang, L. Chen, L. Yue, F. Yang, H. Guo and W. Yang, *J. Alloys Compd.*, 2021, **867**, 158764.

204 S. Li, K. Yang, P. Ye, K. Ma, Z. Zhang and Q. Huang, *Appl. Surf. Sci.*, 2020, **503**, 144090.
205 J. Kim, C. Young, J. Lee, Y.-U. Heo, M.-S. Park, M. S. A. Hossain, Y. Yamauchi and J. H. Kim, *J. Mater. Chem. A*, 2017, **5**, 15065–15072.
206 X. Deng, J. Li, S. Zhu, L. Ma and N. Zhao, *Energy Storage Mater.*, 2019, **23**, 491–498.
207 T. Kshetri, D. D. Khumujam, T. I. Singh, Y. S. Lee, N. H. Kim and J. H. Lee, *Chem. Eng. J.*, 2022, **437**, 135338.
208 D. Xu, Q. Ding, J. Li, H. Chen, Y. Pan and J. Liu, *Inorg. Chem. Commun.*, 2020, **119**, 108141.
209 Y. Pan, Y. Zhao, S. Mu, Y. Wang, C. Jiang, Q. Liu, Q. Fang, M. Xue and S. Qiu, *J. Mater. Chem. A*, 2017, **5**, 9544–9552.
210 S. Xu, R. Liu, X. Shi, Y. Ma, M. Hong, X. Chen, T. Wang, F. Li, N. Hu and Z. Yang, *Electrochim. Acta*, 2020, **342**, 136124.
211 R. Wang, Y. Hu, Z. Pan and J. Wang, *RSC Adv.*, 2020, **10**, 34403–34412.
212 S. Zhang, D. Li, S. Chen, X. Yang, X. Zhao, Q. Zhao, S. Komarneni and D. Yang, *J. Mater. Chem. A*, 2017, **5**, 12453–12461.
213 X. Wang, N. Yang, Q. Li, F. He, Y. Yang, B. Wu, J. Chu, A. Zhou and S. Xiong, *J. Solid State Chem.*, 2019, **277**, 575–586.
214 H. Yi, H. Wang, Y. Jing, T. Peng and X. Wang, *J. Power Sources*, 2015, **285**, 281–290.
215 J. Zhao, M. Wang, S. Wang, S. Zhang, J. Wang, X. Qiao, J. Mi, M. Ge and Y. Feng, *Electrochim. Acta*, 2023, **464**, 142920.
216 J. Gu, L. Sun, Y. Zhang, Q. Zhang, X. Li, H. Si, Y. Shi, C. Sun, Y. Gong and Y. Zhang, *Chem. Eng. J.*, 2020, **385**, 123454.
217 Z. Zhang, H. Huo, J. Gao, Z. Yu, F. Ran, L. Guo, S. Lou, T. Mu, X. Yin and Q. Wang, *J. Alloys Compd.*, 2019, **801**, 158–165.
218 G. Duan, S. Zeng, H. Jin, S. He, H. Yang, X. Han, C. Zhang, Y. Huang and S. Jiang, *Ind. Crops Prod.*, 2024, **222**, 119616.
219 M. G. Tadesse, A. S. Ahmmed and J. F. Lübben, *J. Compos. Sci.*, 2024, **8**, 53.
220 C. Chen, S. Wei, Q. Zhang, H. Yang, J. Xu, L. Chen and X. Liu, *J. Colloid Interface Sci.*, 2024, **664**, 53–62.
221 L. Sajjad, G. Ali, M. A. Mansoor and M. F. Khan, *J. Energy Storage*, 2023, **72**, 108351.
222 D. S. Patil, S. Pawar, R. Devan, S. Mali, M. Gang, Y. Ma, C. Hong, J. Kim and P. Patil, *J. Electroanal. Chem.*, 2014, **724**, 21–28.
223 A. T. Prasannakumar, R. Rohith, V. Manju, R. R. Mohan and S. J. Varma, *J. Energy Storage*, 2024, **76**, 109732.
224 X. Liang, L. Zhao, Q. Wang, Y. Ma and D. Zhang, *Nanoscale*, 2018, **10**, 22329–22334.
225 J. Tian, N. Cui, P. Chen, K. Guo and X. Chen, *J. Mater. Chem. A*, 2021, **9**, 20635–20644.
226 S.-Y. Lee, J.-I. Kim and S.-J. Park, *Energy*, 2014, **78**, 298–303.
227 A. Olad and H. Gharekhani, *Prog. Org. Coat.*, 2015, **81**, 19–26.
228 D. Salinas-Torres, J. M. Sieben, D. Lozano-Castello, D. Cazorla-Amorós and E. Morallón, *Electrochim. Acta*, 2013, **89**, 326–333.
229 Y. Li and C. Chen, *J. Mater. Sci.*, 2017, **52**, 12348–12357.
230 W. Du, X. Wang, X. Sun, J. Zhan, H. Zhang and X. Zhao, *J. Electroanal. Chem.*, 2018, **827**, 213–220.
231 H. Wang and Y. Xie, *J. Energy Storage*, 2022, **52**, 105042.
232 E. Shanmugasundaram, V. Ganesan, V. Narayanan, K. Vellaisamy, N. i. Saleh and S. Thambusamy, *Nanoscale Adv.*, 2024, **6**, 1765–1780.
233 L. S. Ghadimi, N. Arsalani, A. G. Tabrizi, A. Mohammadi and I. Ahadzadeh, *Electrochim. Acta*, 2018, **282**, 116–127.
234 A. Olad and H. Gharekhani, *J. Polym. Res.*, 2016, **23**, 1–11.
235 L. Li, E. Liu, J. Li, Y. Yang, H. Shen, Z. Huang, X. Xiang and W. Li, *J. Power Sources*, 2010, **195**, 1516–1521.
236 Q. Tan, Y. Xu, J. Yang, L. Qiu, Y. Chen and X. Chen, *Electrochim. Acta*, 2013, **88**, 526–529.
237 M. Zhong, Y. Song, Y. Li, C. Ma, X. Zhai, J. Shi, Q. Guo and L. Liu, *J. Power Sources*, 2012, **217**, 6–12.
238 V. K. Pandey, S. Verma and B. Verma, *Chem. Phys. Lett.*, 2022, **802**, 139780.
239 M. Selvakumar, *Int. J. Hydrogen Energy*, 2018, **43**, 4067–4080.
240 A. Chonat and S. Palatty, *Energy Fuels*, 2020, **34**, 10148–10159.
241 H. Wang, J. Xu and Y. Xie, *Appl. Surf. Sci.*, 2023, **637**, 157980.
242 X. Yang, X. Wang, B. Lu, B. Huang, Y. Xia and G. Lin, *Appl. Surf. Sci.*, 2023, **639**, 158191.
243 G. Singh, Y. Kumar and S. Husain, *Energy Technol.*, 2023, **11**, 2200931.
244 Z. Li, S. Bai, K. Chen, Y. Liu, Y. Zhang and S. Liu, *Chem. Eng. J.*, 2024, **481**, 148486.
245 A. K. Ghasemi, M. Ghorbani, M. S. Lashkenari and N. Nasiri, *Electrochim. Acta*, 2023, **439**, 141685.
246 Z. Abbas, M. R. A. Karim, W. Shehzad, N. A. Shama, J. Kumar, S. Karakuş, R. A. Soomro and A. Nafady, *Electrochim. Acta*, 2023, **471**, 143350.
247 M. V. Lebedeva and E. N. Gribov, *Solid State Ionics*, 2023, **401**, 116353.
248 H. Mohamed, M. Abo-Aly, S. A. Wahab, M. Mousa and A. A. Ali, *J. Energy Storage*, 2023, **70**, 108056.
249 X. Tao, S. Ye, K. Zhu, L. Dou, P. Cui, J. Ma, C. Zhao, X. Wei, L. Guo and A. Hojjati-Najafabadi, *ACS Appl. Energy Mater.*, 2023, **6**, 8177–8188.
250 B. Zhou, H. Li, Z. Li, S. Ji, Y. Li, J. Yang and C. Yang, *J. Dispersion Sci. Technol.*, 2023, **44**, 1516–1525.
251 Y. Gogotsi and P. Simon, *Science*, 2011, **334**, 917–918.
252 K. Nasrin, M. Arunkumar, N. K. Kumar, V. Sudharshan, S. Rajasekar, D. Mukhilan, M. Arshad and M. Sathish, *Chem. Eng. J.*, 2023, **474**, 145505.